MODELING PERFORMANCE OF HORIZONTAL WELLS WITH MULTIPLE FRACTURES IN TIGHT GAS RESERVOIRS

A Thesis

by

GUANGWEI DONG

Submitted to the Office of Graduate Studies of
Texas A&M University
in partial fulfillment of the requirements for the degree of

MASTER OF SCIENCE

December 2010

Major Subject: Petroleum Engineering

Modeling Performance of Horizontal Wells with Multiple Fractures

in Tight Gas Reservoirs

MODELING PERFORMANCE OF HORIZONTAL WELLS WITH MULTIPLE FRACTURES IN TIGHT GAS RESERVOIRS

A Thesis

by

GUANGWEI DONG

Submitted to the Office of Graduate Studies of
Texas A&M University
in partial fulfillment of the requirements for the degree of

MASTER OF SCIENCE

Approved by:

Chair of Committee,	Ding Zhu
Committee Members,	Behnam Jafarpour
	Raytcho Lazarov
Head of Department,	Steve Holditch

December 2010

Major Subject: Petroleum Engineering

ABSTRACT

Modeling Performance of Horizontal Wells with Multiple Fractures

in Tight Gas Reservoirs. (December 2010)

Guangwei Dong, B.S., Tsinghua University

Chair of Advisory Committee: Dr. Ding Zhu

Multiple transverse fracturing along a horizontal well is a relatively new technology that is designed to increase well productivity by increasing the contact between the reservoir and the wellbore. For multiple transverse fractures, the performance of the well system is determined by three aspects: the inflow from the reservoir to the fracture, the flow from the fracture to the wellbore, and the inflow from the reservoir to the horizontal wellbore. These three aspects influence each other and combined, influence the wellbore outflow.

In this study, we develop a model to effectively formulate the inter-relationships of a multi-fracture system. This model includes a reservoir model and a wellbore model. The reservoir model is established to calculate both independent and inter-fracture productivity index to quantify the contribution from all fractures on pressure drop of each fracture, by using the source functions to solve the single-phase gas reservoir flow model. The wellbore model is used to calculate the pressure distribution along the wellbore and the relationship of pressure between neighboring fractures, based on the basic pressure drop model derived from the mechanical energy balance. A set of equations with exactly the same number of fractures will be formed to model the system

by integrating the two models. Because the equations are nonlinear, iteration method is used to solve them.

With our integrated reservoir and wellbore model, we conduct a field study to find the best strategy to develop the field by hydraulic fracturing. The influence of reservoir size, horizontal and vertical permeability, well placement, and fracture orientation, type (longitudinal and transverse), number and distribution are completely examined in this study. For any specific field, a rigorous step-by-step procedure is proposed to optimize the field.

DEDICATION

This work is dedicated to my parents, Chuanzhan Dong and Guifen Mu, who taught me everything to be a good person with their endless love. Without them I would be nothing. It is also dedicated to my maternal grandmother who is now in the late period of breast cancer. Hopefully this work and the MS degree give her peace of mind in the last period of her whole life. Also, this work is dedicated to the other three grandparents. I didn't even have a chance to see them because they all died before I was born.

ACKNOWLEDGEMENTS

I would like to thank my committee chair, Dr. Ding Zhu, for all her endless support and help in achieving this degree. I would also like to thank her for her encouraging me to be a good man, for her support in our daily lives to overcome the difficulties of living in a foreign country, and for her welcome at the CAPE new Chinese students party and at the Chinese New Year party at her home, making us feel that it is not only a school, but also a home. She is not only a teacher, but also a mother.

Thanks to Dr. Jafarpour and Dr. Lazarov for serving as my advisory committee member.

Thanks to Jiajing Lin, Xuehao Tan, and Bo Song for their great help during my study.

Thanks to all of my colleagues and friends who share a good time with me and help me in daily life.

Thanks to my mother and father for their encouragement throughout all these years of pursuing a doctoral degree.

Finally, thanks to my maternal grandmother for her endless love for me during her whole life.

TABLE OF CONTENTS

CHAPTER Page

LIST OF FIGURES

Page

LIST OF TABLES

CHAPTER I

INTRODUCTION

1.1 Background

Horizontal and multilateral wells are relatively new technologies in the oil and gas industry compared with the conventional vertical wells. These technologies arise in response to the depletion of conventional resources as the increasing worldwide demand for more oil and gas accelerates the development of unconventional resources, such as heavy oil and low-permeability formations. In the 1980's, the development of horizontal wells improved oil and gas recovery by accessing unconventional resources, increasing the contact between reservoir and wellbore and the productivity per well, reducing the number of wells needed, and thereby reducing the cost of field development. Multilateral wells extend the advantages of single horizontal wells by drilling multiple horizontal laterals starting from the same mother bore, leading to increasing reservoir exposure to wellbore and production. At the same time, the cost of drilling multilateral wells is not proportional to the number of laterals because only one vertical section is needed. Recently, hydraulic fracturing has been applied to horizontal and dual-lateral wells, especially in low-permeability formations. For low-permeability reservoirs, hydraulically created fractures contact more reservoir, significantly improve the flow condition in the reservoir.

This thesis follows the style of *SPE Journal*.

However, as more advanced technologies are developed, the well structure becomes more complex. New theoretical models are needed to study the well performance. In this study, we focus on horizontal wells with multiple transverse fractures in gas reservoirs. The ultimate objective is to develop a method that can evaluate the performance of such a system for different reservoir conditions, and to examine the effect of a multiple fracture system on well performance.

1.2 Literature Review

Many models have been published for horizontal wells before. Joshi (1988) developed a steady-state flow model based on a previous analytical solution. He derived an equation for the flow rate to a horizontal well of length L by adding a solution for the flow resistance in the horizontal plane with the solution for the flow resistance in the vertical plane, taking into the account of vertical-to-horizontal anisotropy. Joshi's model is the one of the first analytical models of horizontal well inflow and is still widely applied. The expression of the model was modified by Economides et al. (1991).

Butler (1994) derived an analytical equation for steady-state fully-penetrating horizontal well located midway between the upper and lower boundaries, based on point source method and the image well superposition solution presented by Muskat (1937).

Furui et al. (2003) developed a simple analytical model for steady-state horizontal well inflow performance. This model incorporates well completion effects and assumes full penetration of the horizontal well to a rectangular reservoir with no-flow boundaries at the top and bottom of the reservoir and constant pressure at the reservoir boundaries in

the y-direction, and that the flow near the well is radial and becomes linear farther from the well. Furui et al.'s model was based on a more physical system and approach, thus it is more reasonable.

Babu and Odeh (1989) developed a pseudo steady-state model of inflow performance. This model presumes that the reservoir is bounded by no-flow boundaries, and is based on radial flow in the y-z plane, with the deviation of the drainage area from a circular shape in this plane accounted for with a geometry factor, and flow from beyond the wellbore in the x-direction accounted for with a penetration skin factor.

For transient flow condition, Ozkan et al. (1989) and Kuchuk et al. (1991) developed their models. Kuchuk et al.'s model will be presented in detail in Chapter II.

The research for performance of horizontal wells with fractures had been conducted. There are analytical models and numerical models. Valko and Amini (2007) developed the method of distributed volumetric sources (DVS) for calculating the transient and pseudo-steady state productivity of complex well-fracture systems. Magalhaes el al. (2007) used DVS method for horizontal wells with single longitudinal fracture. Kamkom (2007) used the two-dimensional source functions to calculate the productivity index of horizontal and slanted wells with the method of Green's source functions to solve the single phase reservoir flow model, and the method of superposition to account for the inter-fracture flow. Lin and Zhu (2010) applied the three-dimensional source function to horizontal gas wells.

The gas reservoir inflow model, a solution of diffusivity equation, is formulated by mass balance, Darcy's law and real gas law, and based on the assumptions of constant

permeability and compressibility factor. For a cylindrical-shaped reservoir with a vertical well in the center, analytical models had been developed (Economides et al., 1993; Hill et al., 2008). However, for a rectangular-shape reservoir with hydraulically fractured horizontal wells, the source function is the only effective analytical approach so far. At the presence of sinks\sources, the diffusivity equation is solved by integrating the source functions in the time and space domain. The specific source functions of some common types of reservoirs, sources and boundary conditions had been formulated. And it had been shown that the source function in the three-dimensional space domain is equal to the product of three one-dimensional source functions for certain conditions, making the solution quite convenient.

1.3 Objectives

The primary objective of this study is to estimate production from hydraulically fractured horizontal wells in low-permeability tight gas reservoirs, especially horizontal wells with multiple transverse fractures. We will study the performance of three completion schemes:

1. Horizontal well with no hydraulic fracturing and openhole completion
2. Horizontal well with multiple transverse fractures and cased/perforated completion
3. Horizontal well with multiple transverse fractures and openhole completion

For the second case, we will perform a complete study and give accurate prediction; and for the third case which is much more complex, we will only give an approximation and

see whether there is improvement compared to the second case, and some tasks will be proposed as recommendations for future work.

We will also study the influence of reservoir, wellbore and fracture parameters to well performance, such as permeability, anisotropic index, wellbore size, fracture geometry, and fracture distribution. Furthermore, we will find the optimum number of fractures for any specific field case. Based on our study, we will provide suggestions and strategies to the choice of technologies of field development.

The methodology includes a reservoir model and a wellbore model. The reservoir model is established using the Green's source functions by Lin and Zhu (2010), and we directly apply the result to this work. The wellbore model, which is the main focus of this study, is used to find the pressure distribution along the wellbore. Different from previous work which treats the pressure distribution along the wellbore as a constant, this study uses the single-phase compressible flow model to calculate the pressure drop between the wellbore segments of neighboring fractures, leading to a nonlinear system with respect to flow rates. We use iteration method to solve the system.

1.4 Organization

This thesis is written in four chapters. In Chapter I, research background and objectives are introduced, and previous work on performance of horizontal wells and hydraulically fractured wells is reviewed. Chapter II identifies three different methods of the field development and their respective flow regimes, derives a rigorous wellbore model which calculates the pressure drop along the wellbore, formulates a multi-fracture system

integrated by the reservoir model and the wellbore model as a set of nonlinear equations, and solves the equations by a well-established iteration method. In Chapter III, a hypothetical case is used to demonstrate the objectives mentioned above, results are presented and analysis is performed. In Chapter IV, conclusions based on the preceding results and discussions are drawn, and recommendations for future work are proposed.

CHAPTER II

THEORETICAL MODEL DEVELOPMENT

2.1 Introduction

In this chapter, we develop a theoretical model to simulate the performance of a multi-fracture system with horizontal wells as shown in Fig. 2.1. The reservoir model is adopted from the source function method by Lin and Zhu (2010), which calculates both the independent and the inter-fracture productivity index to quantify the contributions from all fractures on the pressure drop of each fracture. The wellbore pressure drop model serves a boundary condition of the reservoir model, providing additional constraints to the system equations of reservoir flow.

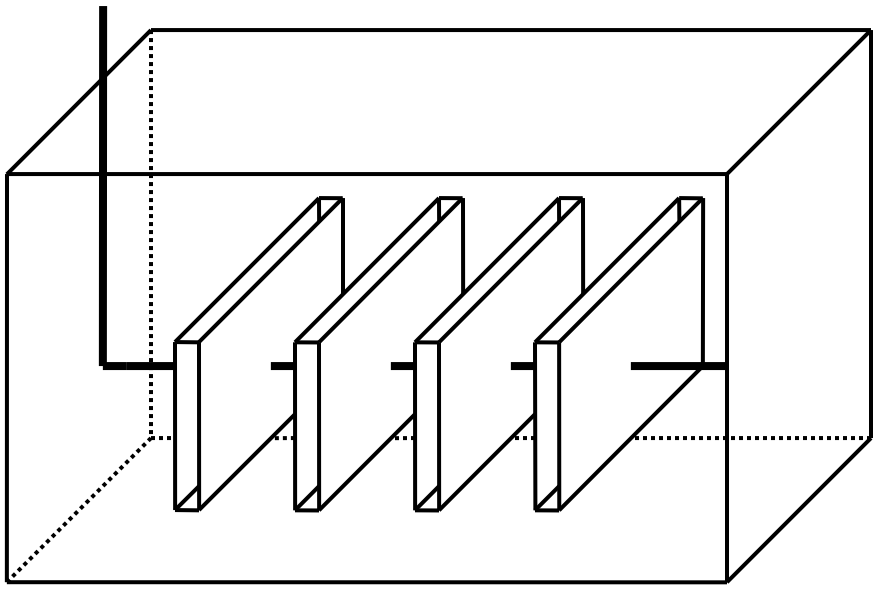

Fig. 2.1 Horizontal well with multiple transverse fractures in a rectangular reservoir

2.2 Structure of Wellbore Completion and Fracture Model

Although there are many types of well completion, in this study we only focus on the ones which are widely used and model the performance under these conditions. There are three conditions we will study: first, unfractured horizontal well with openhole completion; second, fractured horizontal well with cased/perforated completion; third, fractured horizontal well with openhole completion.

The flow regimes of these conditions needs to be carefully identified because flow regimes can be totally different based on different well completion methods and thereby leading to significant difference in well performance. Correctly identifying the flow regimes and selecting appropriate models are important to correctly predict well performance.

For fractured horizontal well with cased/perforated completion, wellbore flow is only contributed by fractures. There is no communication between reservoir and wellbore (Fig. 2.2). In this case, the wellbore is not a source, and the inter-source relationship is only between one fracture and another. The wellbore flow rate is constant along the wellbore, and inflow rate changes when across a fracture. The constant-rate model based on the mechanical energy balance is appropriate for calculating the pressure drop within the segment.

Things become more complex for fractured horizontal well with openhole completion. In this case, wellbore is exposed to reservoir, so inflow inside wellbore is contributed by both fracture and reservoir continuously along the wellbore (Fig. 2.3). Both the wellbore and fractures are sources, the inter-source relationship now

incorporates two parts: fracture-to-fracture relationship, and fracture-to-wellbore relationship. The number of unknown parameters doubles, making the problem big. Also, wellbore flow becomes a function of location. A model that accounts for inflow along the wellbore should be used. We use the model developed by Ouyang et al. (1998) to address this situation rather than the constant-rate model.

For unfractured horizontal well with openhole completion (Fig. 2.4), many models have been established for transient, pseudo steady-state, and steady-state conditions. We use transient flow model by Kuchuk et al. for this study.

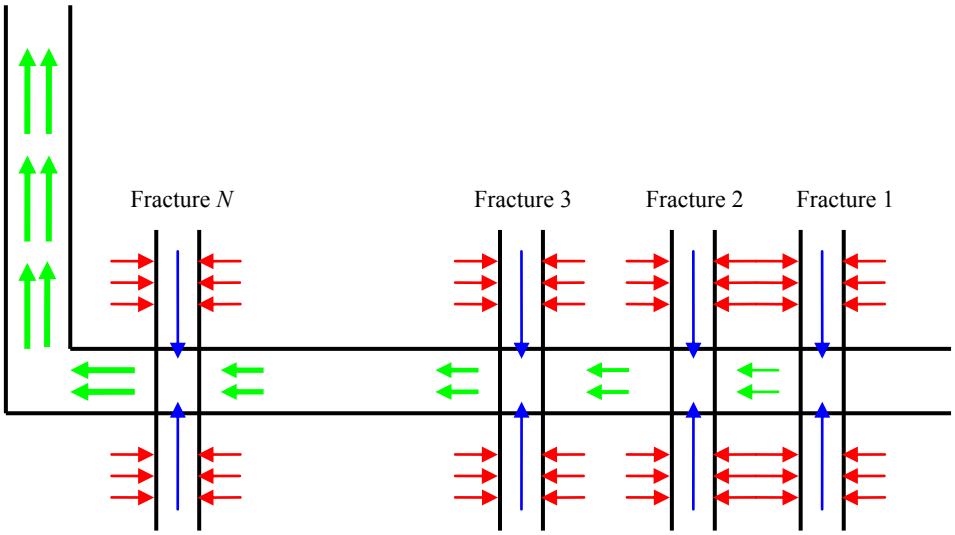

Fig. 2.2 Flow regime of fractured horizontal well with cased/perforated completion

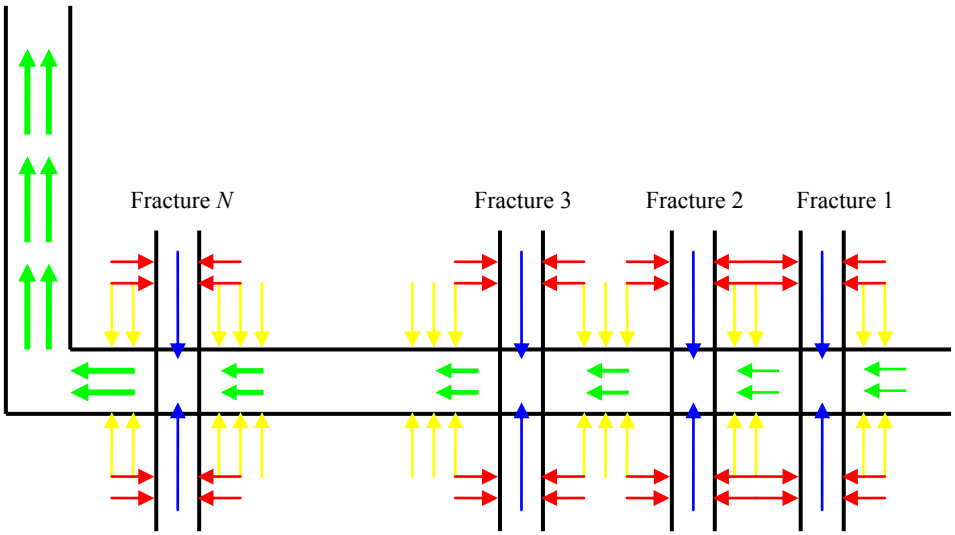

Fig. 2.3 Flow regime of fractured horizontal well with openhole completion

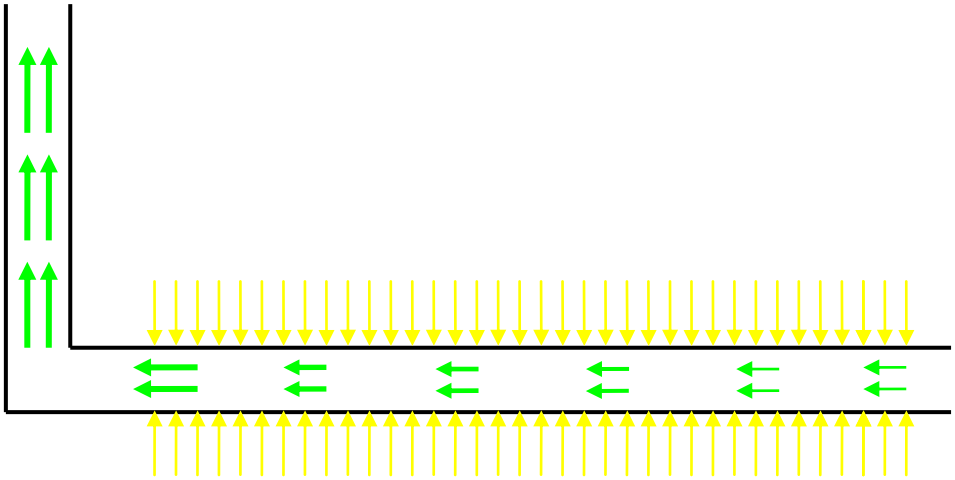

Fig. 2.4 Flow regime of unfractured horizontal well with openhole completion

2.3 Model Development

In this section, we introduce different well completion structures that are commonly used in developing tight gas reservoirs. Completion types are discussed, namely openhole,

slotted liner, and cased/perforated well. Two wellbore pressure drop models, constant rate or varying rate along the wellbore, are derived for appropriate well completion structures. The corresponding integrated solution models are described to solve the specific problem.

2.3.1 Completion Model

Horizontal well completion influences the well performance. The effect can be expressed as a skin factor. In this section, a review of common types of well completions and their respective skin factor model is presented.

Openhole Completions. The openhole completion is common for horizontal wells and multilateral wells. After the borehole is drilled, there is no more completion and the entire wellbore is open to the reservoir. Openhole completion is the simpliest and least expensive. Its use is limited to reservoirs that are strong enough to withstand collapsing stresses. It gives the maximum wellbore-to-reservoir contact assuming that near-wellbore reservoir damage is under control. The only skin factor in a case of openhole completion is damage skin, which can be expressed for horizontal wells as Eq. 2.1

$$s_d^o = \left(\frac{k}{k_s} - 1\right) \ln\left[\frac{1}{I_{ani}+1}\left(\frac{a_{H,\max}}{r_w} + \sqrt{\frac{a_{H,\max}^2}{r_w^2} + I_{ani}^2 + 1}\right)\right] \quad \text{.....(2.1)}$$

where $a_{H,\max}$ is the largest horizontal axis (near the vertical section) of the cone of damage.

Another advantage of openhole completion is that it provides the maximum flexibility for future well modification. For example, a liner with external casing packers can be

installed at a later stage, or an openhole well can be converted to a fully cemented completion.

Slotted Liner Completions. Slotted liner is widely used in horizontal well completions to maintain borehole integrity and prevent sand production. A slotted liner has numerous long and narrow openings, or slots, which are milled into the base pipe to allow fluid to flow into the liner. Slot patterns are characterized by the arrangement of the slots around the circumference of the liner. The slotted liner can be single or multiple, in-line or staggered, as shown in Fig. 2.5.

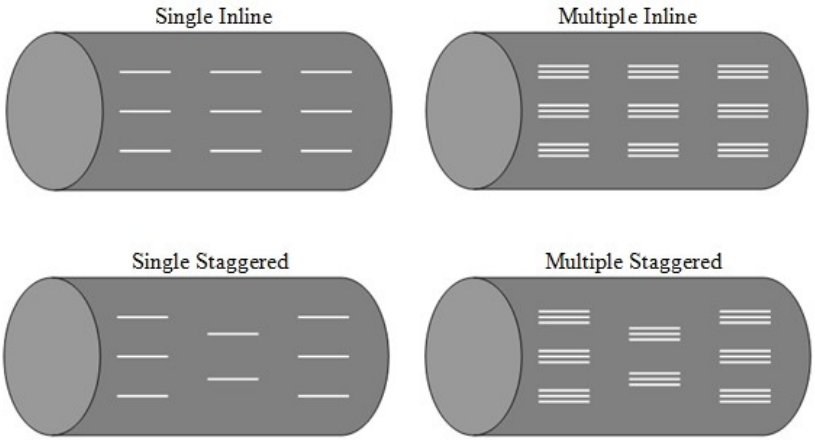

Fig. 2.5 Slot patterns for slotted liner completion

A skin model for slotted liner completions is given as follows (Furui, 2004):

$$s_{SL} = s_{SL}^{0} + f_{tSL} F_{o,w} \quad \text{.....(2.2)}$$

where s_{SL}^{0} is the rate-independent skin

$$s_{SL}^{0} = s_{SL,l}^{0} + s_{SL,r}^{0} \quad \text{.....(2.3)}$$

f_{tSL} is the turbulence scale factor

$$f_{tSL} = f_{tSL,l} + f_{tSL,r} \quad \text{(2.4)}$$

$F_{o,w}$ is the Forchheimer number

$$F_{o,w} = \frac{\beta \rho k}{\mu} \frac{q}{2\pi r_w L} \quad \text{(2.5)}$$

The subscripts l and r denote the linear flow inside the slots and the radial flow outside the liner. Letting k_l be the permeability of the slots, the linear flow components are

$$s^0_{SL,l} = \frac{2\pi}{n_s m_s w_{sD} \lambda} \frac{k}{k_l} t_{sD} \quad \text{(2.6)}$$

$$f_{SL,l} = \left(\frac{2\pi}{n_s m_s w_{sD} \lambda} \right)^2 \frac{\beta_l}{\beta} t_{sD} \quad \text{(2.7)}$$

$$t_{sD} = \frac{t_s}{r_w} \quad \text{(2.8)}$$

Two additional parameters ν and γ determine whether flow convergence in the axial direction along the liner is important, given by

$$\nu = \sin \frac{\pi}{m_s} \quad \text{(2.9)}$$

$$\gamma = \frac{l_{sD}}{2\lambda} \quad \text{(2.10)}$$

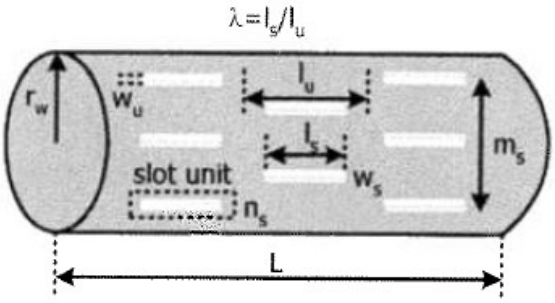

Fig. 2.6 Slotted liner completion skin model

The radial flow components are explained in detail in Furui's original work for skin model. The parameters used in Eqs. 2.6 to 2.10 are illustrated in Fig. 2.6.

Cemented, Cased and Perforated Completions. Perforation is also a practiced method for horizontal well. It is a series of communication tunnel extending beyond the casing or liner into the reservoir formation for a cased and cemented wellbore. A longer penetration is always expected to create effective flow communication to the part of the formation that has not been damaged by drilling or completion. The perforation shot density is the number of perforations per liner foot (spf). In general, productivity is improved with shot density increases. Perforation phasing is the radial distribution of successive perforating charges around the circumference of the casing of liner. The process of perforating produces a crushed zone around the perforation in which permeability can be reduced. Estimates suggest that permeability in the compacted zone is about 20% of the original and can be a serious impediment to productivity. The perforation skin model given below is based on Furui's model, which deconstructs the

skin factor into three components: the 2D convergence skin, s_{2D}; the wellbore blockage skin, s_{wb}; and the 3D convergence skin, s_{3D}.

The skin equation for 2D convergence is

$$s_{2D} = \begin{cases} a_m \ln\frac{4}{l_{pD}} + (1-a_m)\ln\frac{4}{1+l_{pD}} + \ln\frac{\sqrt{k_y/k_z}+1}{2\left(\cos^2\alpha + \sqrt{k_y/k_z}\sin^2\alpha\right)^{0.5}} & m = 1,2 \\ a_m \ln\frac{4}{l_{pD}} + (1-a_m)\ln\frac{4}{1+l_{pD}} & m = 3,4 \end{cases} \quad \text{……..…….(2.11)}$$

where m is the number of perforations in the y-z plane, α is the perforation orientation, and

$$l_{pD} = \frac{l_p}{r_w} \text{ ……..…….....…….....……...(2.12)}$$

The wellbore blockage skin factor is

$$s_{wb} = b_m \ln\left[\frac{c_m}{l_{pD,eff}} + \exp\left(-\frac{c_m}{l_{pD,eff}}\right)\right] \text{ ……..…….....……...(2.13)}$$

where

$$l_{pD,eff} = \begin{cases} l_{pD}\left[\frac{(k_y/k_z)\sin^2\alpha + \cos^2\alpha}{(k_y/k_z)\cos^2\alpha + \sin^2\alpha}\right]^{0.675} & m = 1 \\ l_{pD}\left[\frac{1}{(k_y/k_z)\cos^2\alpha + \sin^2\alpha}\right]^{0.675} & m = 2 \\ l_{pD} & m = 3,4 \end{cases} \quad \text{…..…….....…….....……...(2.14)}$$

The skin equation for 3D convergence is

$$s_{3D} = 10^{\beta_1} x_{pD}^{\beta_2 - 1} r_{pD}^{\beta_2} \quad \text{.....(2.15)}$$

where

$$\beta_1 = d_m \log r_{pD} + e_m \quad \text{.....(2.16)}$$

$$\beta_2 = f_m r_{pD} + g_m \quad \text{.....(2.17)}$$

$$x_{pD} = \begin{cases} \dfrac{x_p}{l_p \sqrt{\left(k_x / k_z\right) \sin^2 \alpha + \left(k_x / k_y\right) \cos^2 \alpha}} & m = 1,2 \\ \dfrac{x_p}{l_p} \left(\dfrac{\sqrt{k_y k_z}}{k_x} \right)^{0.5} & m = 3,4 \end{cases} \quad \text{.....(2.18)}$$

$$r_{pD} = \begin{cases} \dfrac{r_p}{2x_p} \left[1 + \cos\left(\alpha'' - \alpha'\right) \sqrt{\dfrac{k_x}{k_y} \sin^2 \alpha + \dfrac{k_x}{k_z} \mathrm{s} \cos^2 \alpha} \right] & m = 1,2 \\ \dfrac{r_p}{2x_p} \left[1 + \left(\dfrac{k_x}{\sqrt{k_y k_z}} \right)^{0.5} \right] & m = 3,4 \end{cases} \quad \text{.....(2.19)}$$

$$\alpha' = \arctan\left(\sqrt{k_y / k_z} \tan \alpha \right) \quad \text{.....(2.20)}$$

$$\alpha'' = \arctan\left(\sqrt{k_z / k_y} \tan \alpha \right) \quad \text{.....(2.21)}$$

The total skin factor caused by a cased/perforated completion in a horizontal lateral is

$$s_p^o = s_{2D} + s_{wb} + s_{3D} \quad \text{.....(2.22)}$$

The perforation completion skin factor including formation damage effect is

$$s_p = s_d^o + \frac{k}{k_s} s_p^o + \frac{\beta_s}{\beta} f_{tp} F_{o,w} \quad \text{.....(2.23)}$$

where s_d^o is the local damage skin given by Eq. 2.1.

2.3.2 Wellbore Model

In the case of fractured horizontal well with cased/perforated well completion, the flow within each segment of wellbore between two neighboring fractures keep constant except for the locations wellbore is going across a fracture (Fig. 2.7). Therefore, we can apply the constant-rate model for single-phase flow, which is derived from the mechanical energy balance (Economides et al., 1993), to each of the wellbore segment. The mechanical energy balance is

$$\frac{dp}{\rho}+\frac{udu}{g_c}+\frac{gdz}{g_c}+\frac{2f_f u^2 dL}{g_c D}+dW_s=0 \quad \text{.....(2.24)}$$

where the second to fifth term on the LHS represents the influence of kinetic energy, potential energy, friction, and shaft work in the pipeline to the overall pressure drop, respectively.

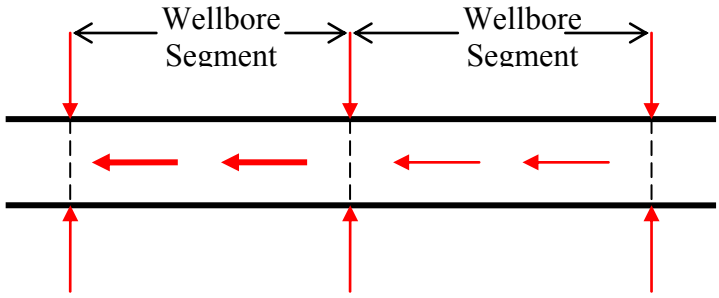

Fig. 2.7 Schematic of point inflow for constant-rate model

Assume that there's no shaft work device and kinetic energy changes (not considering kinetic energy change might lead to certain error, but we simply the problem in this wayfor the convenience of model derivation), Eq. 2.24 is simplified to

$$\frac{dp}{\rho}+\left(\frac{g}{g_c}\sin\theta+\frac{2f_f u^2 dL}{g_c D}\right)=0 \quad \text{.....(2.25)}$$

For a gas well, from the real gas law, the density is expressed as

$$\rho=\frac{pMW}{ZRT}=\frac{28.97\gamma_g p}{ZRT} \quad \text{.....(2.26)}$$

The velocity can be written in terms of the volumetric flow rate at standard conditions, q

$$u=\frac{4}{\pi D^2}qB_g \quad \text{.....(2.27)}$$

$$B_g=Z\frac{T}{T_{sc}}\frac{p_{sc}}{p} \quad \text{.....(2.28)}$$

Substituting Eq. 2.28 into Eq. 2.27 yields

$$u=\frac{4}{\pi D^2}qZ\frac{T}{T_{sc}}\frac{p_{sc}}{p} \quad \text{.....(2.29)}$$

Substituting Eqs. 2.26 and 2.29 into Eq. 2.25 yields

$$\frac{ZRT}{28.97\gamma_g p}dp+\left[\frac{g}{g_c}\sin\theta+\frac{32f_f}{\pi^2 g_c D^5}\left(\frac{ZTqp_{sc}}{pT_{sc}}\right)^2\right]dL=0 \quad \text{.....(2.30)}$$

Eq. 2.30 still contains three variables that are functions of position: the compressibility factor Z, temperature T, and pressure p. To solve Eq. 2.30 rigorously, the temperature profile can be provided and the compressibility factor replaced by a function of temperature and pressure using an equation of state. This approach requires numerical integration.

Alternatively, single values of average of temperature and compressibility factor over the segment of pipe of interest can be assumed. Our derivation uses this approach.

We can use either arithmetic mean temperature

$$\bar{T} = \left(T_1 + T_2\right)/2 \quad \text{.....(2.31)}$$

or log-mean temperature (Bradley, 1987)

$$\bar{T} = \frac{T_2 - T_1}{\ln\left(T_2 / T_1\right)} \quad \text{.....(2.32)}$$

An estimate of the average compressibility factor $\bar{Z}$, can be obtained as a function of average temperature $\bar{T}$, and the known upstream pressure p_1. On the downstream pressure p_2 has been calculated, $\bar{Z}$ can be checked using $\bar{T}$ and the mean pressure $\left(p_1 + p_2\right)/2$. If the new estimate differs significantly, the pressure calculation can be repeated using a new estimate of $\bar{Z}$ until the error is less than certain tolerance.

Rearranging Eq. 2.30, we have

$$\frac{ZRT}{2\left(28.97\gamma_g\right)\left(g/g_c\right)\sin\theta}dp^2 + p^2 dL + \frac{32 f_f}{\pi^2 D^5 g \sin\theta}\left(\frac{ZTqp_{sc}}{T_{sc}}\right)^2 dL = 0 \quad \text{.....(2.33)}$$

For convenience, let

$$a = \frac{2\left(28.97\gamma_g\right)\left(g/g_c\right)\sin\theta}{ZRT} \quad \text{.....(2.34)}$$

Substituting Eq. 2.34 into Eq. 2.33 and multiplying both sides by e^{aL} yields

$$e^{aL}dp^2 + p^2 a e^{aL} dL + \frac{32 f_f}{\pi^2 D^5 g \sin\theta}\left(\frac{ZTqp_{sc}}{T_{sc}}\right)^2 a e^{aL} dL = 0 \quad \text{.....(2.35)}$$

Rearranging yields

$$d\left(p^2 e^{aL}\right) + \frac{32 f_f}{\pi^2 D^5 g \sin\theta}\left(\frac{ZTqp_{sc}}{T_{sc}}\right)^2 de^{aL} = 0 \quad \text{.....(2.36)}$$

Integrating using average temperature and compressibility factor gives

$$p_2^2 e^{\bar{a}L} - p_1^2 + \frac{32 f_f}{\pi^2 D^5 g \sin\theta}\left(\frac{\overline{ZT} q p_{sc}}{T_{sc}}\right)^2 \left(e^{\bar{a}L} - 1\right) = 0 \quad \text{.....(2.37)}$$

where

$$\bar{a} = \frac{2\left(28.97\gamma_g\right)\left(g/g_c\right)\sin\theta}{\overline{ZT}R} \quad \text{.....(2.38)}$$

Rearranging yields

$$p_2^2 = e^s p_1^2 - \frac{32 f_f}{\pi^2 D^5 g \sin\theta}\left(\frac{\overline{ZT} q p_{sc}}{T_{sc}}\right)^2 \left(1 - e^s\right) \quad \text{.....(2.39)}$$

where

$$s = -\bar{a}L = \frac{2\left(28.97\gamma_g\right)\left(g/g_c\right)L\sin\theta}{\overline{ZT}R} \quad \text{.....(2.40)}$$

Eqs. 2.39 and 2.40 give the explicit expression for the downstream pressure, p_2, for vertical or inclined wells.

For horizontal wells, $\theta = 0$. So Eq. 2.30 is simplified to

$$\frac{ZRT}{28.97\gamma_g p} dp + \frac{32 f_f}{\pi^2 g_c D^5}\left(\frac{ZTqp_{sc}}{pT_{sc}}\right)^2 dL = 0 \quad \text{.....(2.41)}$$

Multiplying both sides by p^2 yields

$$\frac{pdp}{28.97\gamma_g} + \frac{32 f_f ZT}{\pi^2 D^5 g_c R}\left(\frac{p_{sc} q}{T_{sc}}\right)^2 dL = 0 \quad \text{.....(2.42)}$$

Integrating Eq. 2.42 using average temperature and compressibility factor and rearranging gives

$$p_2^2 = p_1^2 - \frac{64\left(28.97\gamma_g\right) f_f \overline{ZT}}{\pi^2 D^5 g_c R}\left(\frac{p_{sc} q}{T_{sc}}\right)^2 L \quad \text{.....(2.43)}$$

Eq. 2.43 gives the explicit expression for the downstream pressure, p_2, for horizontal wells.

To complete the calculation, the friction factor must be obtained from the Reynolds number and the pipe roughness. We use the explicit Chen equation (Chen, 1979)

$$\frac{1}{\sqrt{f_f}} = -4\log\left\{\frac{\varepsilon}{3.7065} - \frac{5.0452}{N_{\mathrm{Re}}}\log\left[\frac{\varepsilon^{1.1098}}{2.8257} + \left(\frac{7.149}{N_{\mathrm{Re}}}\right)^{0.8981}\right]\right\} \quad \text{.....(2.44)}$$

The Reynolds number N_{Re} is calculated based on standard conditions as the following procedure:

$$N_{\mathrm{Re}} = \frac{Du\rho}{\mu} \quad \text{.....(2.45)}$$

Substituting Eqs. 2.26 and 2.29 into Eq. 2.45 and manipulating yields

$$N_{\mathrm{Re}} = \frac{4\left(28.97\gamma_g\right) q p_{sc}}{\pi D \bar{\mu} R T_{sc}} \quad \text{.....(2.46)}$$

The viscosity $\bar{\mu}$ is calculated at the average temperature and pressure similar to the procedure calculating the compressibility factor $\bar{Z}$.

In oilfield units, Eqs. 2.39, 2.40, 2.43, and 2.46 can be expressed as

$$N_{\mathrm{Re}} = 20.09\frac{\gamma_g q}{D\bar{\mu}} \quad \text{.....(2.47)}$$

For vertical or inclined wells:

$$p_2^2 = e^s p_1^2 - 2.685\times10^{-5}\frac{f_f}{D^5\sin\theta}\left(\frac{\overline{ZT}qp_{sc}}{T_{sc}}\right)^2\left(1-e^s\right) \quad \text{.....(2.48)}$$

where

$$s = -\frac{0.0375\gamma_g L\sin\theta}{\overline{ZT}} \quad \text{.....(2.49)}$$

For horizontal wells:

$$p_1^2 - p_2^2 = 1.007\times10^{-4}\frac{\gamma_g f_f \overline{ZT}q^2 L}{D^5} \quad \text{.....(2.50)}$$

where p is in psia, q is in MSCF/d, D is in inch, L is in ft, μ is in cp, T is in $^\circ R$, and all other variables are dimensionless.

In the case of openhole completion, oil and gas can directly flow from reservoir into wellbore, and flow in the wellbore is changing everywhere (Fig. 2.8). Ouyang et al.'s single-phase model is effective in addressing this situation which accounts for pressure drop caused by inflow and perforation roughness by applying an empirical friction factor correlation.

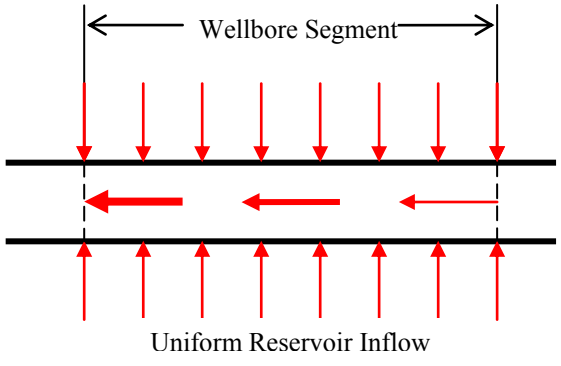

Fig. 2.8 Schematic of uniform reservoir inflow for Ouyang et al.'s model

For a horizontal well segment with a uniform inflow per unit length q_I, Ouyang et al.'s model can be expressed as

$$p_1^2 - p_2^2 = \frac{2 f_f^* \rho u^2 L_s}{g_c d} + \frac{8 \rho u q_I L_s}{\pi g_c d^2} \quad \text{(2.51)}$$

where

$$q_I = \frac{q}{L_s} \quad \text{(2.52)}$$

For laminar flow the friction factor f_f^* is defined as

$$f_f^* = \frac{16}{N_{\mathrm{Re}}}\left(1 + 0.04304 N_{\mathrm{Re},w}^{0.6142}\right) \quad \text{(2.53)}$$

For turbulent flow

$$f_f^* = f_f\left(1 - 0.0153 N_{\mathrm{Re},w}^{0.3978}\right) \quad \text{(2.54)}$$

f_f in Eq. 2.54 is the usual friction factor in Eq. 2.44. $N_{\mathrm{Re},w}$ in Eqs. 2.53 and 2.54 is the inflow Reynolds number, expressed as

$$N_{\mathrm{Re},w} = \frac{q_I \rho}{\pi \mu} \quad \text{(2.55)}$$

N_{Re} is the usual pipe flow Reynolds number

$$N_{\mathrm{Re}} = \frac{D u \rho}{\mu} \quad \text{(2.56)}$$

The axial velocity *u* is the mean velocity in the segment

$$u = \frac{4\bar{q}}{\pi D^2} \quad \text{(2.57)}$$

where

$$\bar{q} = q + \frac{L_s}{2} q_I \quad \text{.....(2.58)}$$

2.3.3 Integrated Model Solution

In this section, we develop methods for solving systems with multiple transverse fractures under the condition of either cased/perforated or openhole completion.

The very first thing is to determine the number of unknown parameters for each system. The unknowns are the flow rates and pressures at the center of sources, so we need to determine, for a given system, how the sources are characterized.

Cased/perforated/fractured. Under the condition of cased/perforated completion, wellbore flow is only contributed by fracture. In the wellbore model, we set the wellbore inflow where other than fracture locations to be zero (Fig. 2.9). Therefore, the number of sources equals to the number of fractures, and all of the unknowns are fracture inflow and fracture pressure. The system can be formulated as Eq. 2.59.

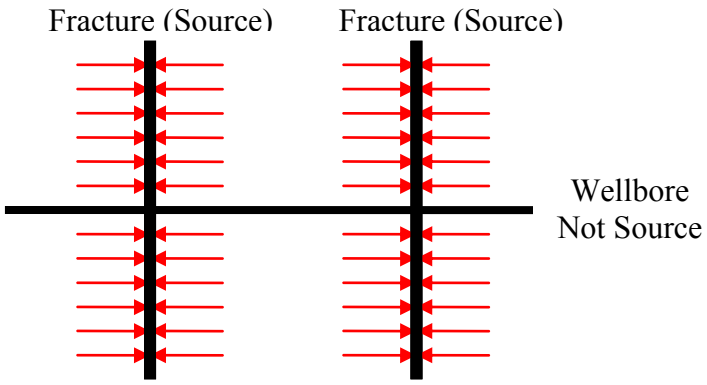

Fig. 2.9 Sources identification for cased/perforated completion

$$\begin{bmatrix} A_{11} & A_{12} & A_{13} & \cdots & A_{1N} \\ A_{21} & A_{22} & A_{23} & \cdots & A_{2N} \\ A_{31} & A_{32} & A_{33} & \cdots & A_{3N} \\ \vdots & \vdots & \vdots & \ddots & \vdots \\ A_{N1} & A_{N2} & A_{N3} & \cdots & A_{NN} \end{bmatrix} \begin{bmatrix} q_1 \\ q_2 \\ q_3 \\ \vdots \\ q_N \end{bmatrix} = \begin{bmatrix} p_e^2 - p_1^2 \\ p_e^2 - p_2^2 \\ p_e^2 - p_3^2 \\ \vdots \\ p_e^2 - p_N^2 \end{bmatrix} \quad \text{.....(2.59)}$$

where A_{ij} is the productivity index calculated by the reservoir model. There are $2N-1$ unknowns, i.e. q_1, q_2, q_3, … , q_N; p_2, … , p_N. Eq. 2.59 provides N equations; the remaining $N-1$ equations will be provided by Eq. 2.60, the wellbore flow equations.

For the last fracture towards the toe of the wellbore (Fracture *1*), since there's no fracture and no flow in the upstream direction, there's no pressure drop in the upstream wellbore segment, and the pressure of this fracture, p_1, equals to the pressure of the wellbore toe. Flow in the wellbore segment between Fracture *1* and its neighboring fracture (Fracture *2*) is q_1, and the pressure drop within this segment is only related with q_1. Similarly, flow within the segment between Fracture *K* and Fracture *K+1* is $q_1 + q_2 + \ldots + q_K$, and the pressure drop within this segment is related with flow from all of the upstream fractures. Therefore, the wellbore pressure drop between any neighboring fractures can be formulated as

$$p_K^2 - p_{K+1}^2 = 1.007\times10^{-4}\frac{\gamma_g f_f \left(\sum_{i=1}^{K} q_i\right)^2 \left(\overline{ZTL}\right)_K}{D^5},\ \left(i=1,2,3,\ldots,N-1\right) \text{.....(2.60)}$$

For convenience, express the RHS of Eq. 2.60 as a function of total flow

$$Dp_i\left(q\right) = 1.007\times10^{-4}\frac{\gamma_g f_f \left(\overline{ZTL}\right)_i}{D^5} q^2 \text{.....(2.61)}$$

Substituting Eqs. 2.60 and 2.61 into Eq. 2.59 yields

$$\begin{bmatrix} A_{11} & A_{12} & A_{13} & \cdots & A_{1N} \\ A_{21} & A_{22} & A_{23} & \cdots & A_{2N} \\ A_{31} & A_{32} & A_{33} & \cdots & A_{3N} \\ \vdots & \vdots & \vdots & \ddots & \vdots \\ A_{N1} & A_{N2} & A_{N3} & \cdots & A_{NN} \end{bmatrix} \begin{bmatrix} q_1 \\ q_2 \\ q_3 \\ \vdots \\ q_N \end{bmatrix} = \begin{bmatrix} p_e^2 - p_1^2 \\ p_e^2 - p_1^2 + Dp_1(q_1) \\ p_e^2 - p_1^2 + Dp_1(q_1) + Dp_2(q_1 + q_2) \\ \vdots \\ p_e^2 - p_1^2 + Dp_1(q_1) + \ldots + Dp_{N-1}\left(\sum_{i=1}^{N-1} q_i\right) \end{bmatrix}$$

……..……...…….....(2.62)

Rearranging both sides yields

$$\begin{cases} A_{11}q_1 + A_{12}q_2 + \ldots + A_{1N}q_N - \left(p_e^2 - p_1^2\right) = 0 \\ A_{21}q_1 + A_{22}q_2 + \ldots + A_{2N}q_N - \left(p_e^2 - p_1^2\right) - Dp_1(q_1) = 0 \\ A_{31}q_1 + A_{32}q_2 + \ldots + A_{3N}q_N - \left(p_e^2 - p_1^2\right) - Dp_1(q_1) - Dp_2(q_1 + q_2) = 0 \\ \vdots \\ A_{N1}q_1 + A_{N2}q_2 + \ldots + A_{NN}q_N - \left(p_e^2 - p_1^2\right) - Dp_1(q_1) - \ldots - Dp_{N-1}\left(\sum_{i=1}^{N-1} q_i\right) = 0 \end{cases}$$

……...……....(2.63)

Denote

$$\vec{q} = \left(q_1, q_2, \ldots, q_N\right)^T$$ ……..……..(2.64)

$$\vec{F} = \left(f_1(\vec{q}), f_2(\vec{q}), \ldots, f_N(\vec{q})\right)^T$$ ……..……...…(2.65)

$$\begin{cases} f_1(\vec{q}) = A_{11}q_1 + A_{12}q_2 + \ldots + A_{1N}q_N - \left(p_e^2 - p_1^2\right) \\ f_2(\vec{q}) = A_{21}q_1 + A_{22}q_2 + \ldots + A_{2N}q_N - \left(p_e^2 - p_1^2\right) - \Delta p_1(q_1) \\ \vdots \\ f_N(\vec{q}) = A_{N1}q_1 + A_{N2}q_2 + \ldots + A_{NN}q_N - \left(p_e^2 - p_1^2\right) - \Delta p_1(q_1) - \ldots - \Delta p_{N-1}\left(\sum_{i=1}^{N-1} q_i\right) \end{cases}$$

……...…….....(2.66)

Then Eq. 2.63 can be expressed in the simple form

$$\vec{F}(\vec{q}) = 0 \quad \text{.....(2.67)}$$

Eq. 2.67 is nonlinear with respect to $\vec{q}$. It can be solved using the Newton-Raphson iteration method, which is an efficient method for solving an equation system, especially for nonlinear equations. It can be seen as an extension of the Newton-Raphson method for single equation. Fundamentals of Newton-Raphson iteration method are given as below (Kincaid and Cheney, 1991)

Expand each f_i of $\vec{F}$ using Taylor series, we have

$$f_i(\vec{q}) \approx f_i\left(\vec{q}^{(k)}\right) + \frac{\partial f_i}{\partial q_1}\left(\vec{q}^{(k)}\right)\left(q_1 - q_1^{(k)}\right) + \ldots + \frac{\partial f_i}{\partial q_N}\left(\vec{q}^{(k)}\right)\left(q_N - q_N^{(k)}\right) \quad \text{.....(2.68)}$$

where $\vec{q}^{(k)}$ represents the value of $\vec{q}$ at the *k*th step.

In vector form

$$\vec{F}(\vec{q}) \approx \vec{F}\left(\vec{q}^{(k)}\right) + \vec{F}'\left(\vec{q}^{(k)}\right)\left(\vec{q} - \vec{q}^{(k)}\right) \quad \text{.....(2.69)}$$

Here $\vec{F}'\left(\vec{q}^{(k)}\right)$ represents the Jacobian matrix of $\vec{F}$ at $\vec{q}^{(k)}$,

$$\vec{F}'\left(\vec{q}^{(k)}\right) = \begin{bmatrix} \frac{\partial f_1}{\partial q_1} & \frac{\partial f_1}{\partial q_2} & \cdots & \frac{\partial f_1}{\partial q_N} \\ \frac{\partial f_2}{\partial q_1} & \frac{\partial f_2}{\partial q_2} & \cdots & \frac{\partial f_2}{\partial q_N} \\ \vdots & \vdots & \ddots & \vdots \\ \frac{\partial f_N}{\partial q_1} & \frac{\partial f_N}{\partial q_N} & \cdots & \frac{\partial f_N}{\partial q_N} \end{bmatrix} \left(\vec{q}^{(k)}\right) \quad \text{.....(2.70)}$$

If the root of the LHS of Eq. 2.69 is $\vec{q}^{*}$, then

$$f_i\left(\vec{q}^{*}\right) = 0 \quad \text{.....(2.71)}$$

Therefore, we treat the vector which makes the RHS of Eq. 2.71 to be zero as a new approximation of $\vec{q}^*$, denoted as $\vec{q}^{(k+1)}$, namely

$$\vec{q}^{(k+1)} = \vec{q}^{(k)} - \left(\vec{F}'\left(\vec{q}^{(k)}\right)\right)^{-1} \vec{F}\left(\vec{q}^{(k)}\right) \quad \text{.....(2.72)}$$

which is the scheme of Newton-Raphson method.

The procedure of Newton-Raphson Iteration is as follow:

(1) Assign an initial value $\vec{q}^{(0)}$ for $\vec{q}$.

(2) For $k = 1, 2, 3, \ldots$, first solve

$$\vec{F}'\left(\vec{q}^{(k)}\right)\delta\vec{q}^{(k)} = \vec{F}\left(\vec{q}^{(k)}\right) \quad \text{.....(2.73)}$$

After solving $\delta\vec{q}^{(k)}$, let

$$\vec{q}^{(k+1)} = \vec{q}^{(k)} + \delta\vec{q}^{(k)} \quad \text{.....(2.74)}$$

Here $\vec{F}'\left(\vec{q}^{(k)}\right)$ is calculated by perturbation method.

$$\frac{\partial f_i}{\partial q_j}\left(\vec{q}\right) = \frac{f_i\left(q_1, \ldots, q_{j-1}, q_j + \Delta q_j, q_{j+1}, \ldots, q_N\right) - f_i\left(q_1, \ldots, q_{j-1}, q_j, q_{j+1}, \ldots, q_N\right)}{\Delta q_j} \quad (2.75)$$

(3) If $\vec{q}^{(k)}$ and $\vec{q}^{(k+1)}$ satisfy certain requirement, like $\left|\vec{q}^{(k+1)} - \vec{q}^{(k)}\right| < \varepsilon$, stop;

otherwise, $k+1 \to k$, and go to (2).

Openhole/fractured. Under the case of openhole completion, all of the wellbore segments between neighboring fractures, includes the segment between the last fracture and the wellbore toe, and the segment between the first fracture and the wellbore heel, serve as sources (Fig. 2.10). There are *N+1* segments, in addition to the *N* fractures, there are 2*N+1* sources in total. The unknown parameters we need to find are the flow

and pressure at the center of each of the sources, $4N+2$ in total. Also, within each wellbore segment, we apply Ouyang et al.'s model to account for the inflow. The formulation of this case is

$$\begin{bmatrix} A_{11} & A_{12} & A_{13} & \cdots & A_{1,2N+1} \\ A_{21} & A_{22} & A_{23} & \cdots & A_{2,2N+1} \\ A_{31} & A_{32} & A_{33} & \cdots & A_{3,2N+1} \\ \vdots & \vdots & \vdots & \ddots & \vdots \\ A_{2N+1,1} & A_{2N+1,2} & A_{2N+1,3} & \cdots & A_{2N+1,2N+1} \end{bmatrix} \begin{bmatrix} q_1 \\ q_2 \\ q_3 \\ \vdots \\ q_{2N+1} \end{bmatrix} = \begin{bmatrix} p_e^2 - p_1^2 \\ p_e^2 - p_2^2 \\ p_e^2 - p_3^2 \\ \vdots \\ p_e^2 - p_{2N+1}^2 \end{bmatrix} \quad \text{.....(2.76)}$$

Eq. 2.76 provides $2N+1$ equations, the remaining are provided by the pressure drop calculation between the center of neighboring sources. Similar to the solution of Eq. 2.59, we use the New-Raphson iteration method to solve Eq. 2.76.

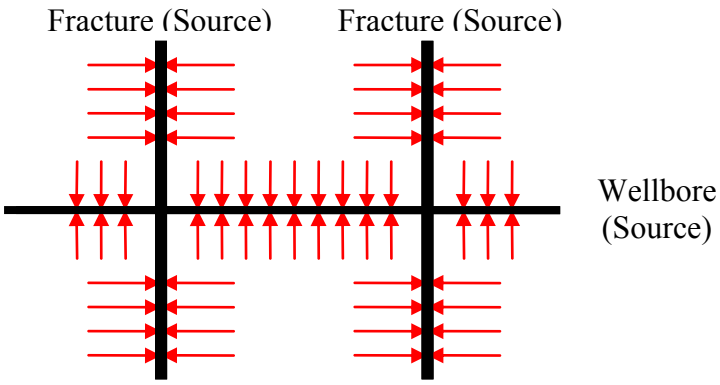

Fig. 2.10 Sources identification for openhole completion

2.3.4 Unfractured Horizontal Gas Well Inflow Model

Many models have been established for unfractured horizontal gas well inflow under transient, pseudo steady-state, or steady-state conditions. In this section, we present

some popular well-established models. But for calculation of unfractured horizontal gas well inflow, we will focus on the models based on transient flow condition, because the use of source functions for fractured horizontal well is based on transient flow and comparison is only valid for the same condition.

For steady-state flow, we have Eq. 2.77 (Furui et al., 2003)

$$q_g = \frac{\sqrt{k_y k_z}\,L\left(p_e^2 - p_{wf}^2\right)}{1424\bar{Z}\bar{\mu}_g T\left(\ln\frac{I_{ani}h}{r_w\left(I_{ani}+1\right)} + \frac{\pi y_b}{I_{ani}h} - 1.224 + s\right)} \quad \text{.....(2.77)}$$

For pseudo steady-state flow, we have Eq. 2.77 (Babu and Odeh, 1989)

$$q_g = \frac{b\sqrt{k_y k_z}\left(\bar{p}^2 - p_{wf}^2\right)}{1424\bar{Z}\bar{\mu}_g T\left(\ln\frac{A^{0.5}}{r_w} + \ln C_H - 0.75 + s_R + \frac{b}{L}s\right)} \quad \text{.....(2.78)}$$

For transient flow, we have

For first radial period that

$$t < \frac{\phi\bar{\mu}_g c_t}{0.0002637\pi k_V}\min\left\{z_w^2, \left(h - z_w\right)^2\right\} \quad \text{.....(2.79)}$$

we have

$$q_g = \frac{2\sqrt{k_H k_V}\,L_{1/2}\left(p_i^2 - p_{wf}^2\right)}{1639.8\bar{Z}\bar{\mu}_g T\left[\log\frac{\sqrt{k_H k_V}\,t}{\phi\bar{\mu}_g c_t r_w^2} - 3.2275 + 0.8686s - 2\log\left[\frac{1}{2}\left(\sqrt[4]{\frac{k_H}{k_V}} + \sqrt[4]{\frac{k_V}{k_H}}\right)\right]\right]}$$

.....(2.80)

For second radial period that

$$\frac{\phi\bar{\mu}_g c_t}{0.0002637\pi k_V}\min\left\{z_w^2, \left(h - z_w\right)^2\right\} < t < \frac{\phi\bar{\mu}_g c_t}{0.0002637\pi k_V}\max\left\{z_w^2, \left(h - z_w\right)^2\right\} \quad \text{...(2.81)}$$

we have

$$q_g = \frac{\sqrt{k_H k_V}\, L_{1/2}\left(p_i^2 - p_{wf}^2\right)}{1639.8\bar{Z}\bar{\mu}_g T\left[\log\frac{\sqrt{k_H k_V}\, t}{\phi\bar{\mu}_g c_t r_w^2} - 3.2275 + 0.4343s - \log\left[\left(1+\sqrt{\frac{k_H}{k_V}}\right)\frac{z_w}{r_w}\right]\right]} \quad \text{.....(2.82)}$$

For intermediate-time linear period that

$$\frac{\phi\bar{\mu}_g c_t h^2}{0.0002637 k_V} < t < \frac{\phi\bar{\mu}_g c_t L_{1/2}^2}{0.0002637 k_H} \quad \text{……..……...…(2.83)}$$

we have

$$q_g = \frac{p_i^2 - p_{wf}^2}{1424\bar{Z}\bar{\mu}_g T\left[\frac{4.064}{141.2hL_{1/2}}\sqrt{\frac{t}{\phi\bar{\mu}_g c_t k_H}} + \frac{s_z}{k_H h} + \frac{s}{2L_{1/2}\sqrt{k_H k_V}}\right]} \quad \text{……....(2.84)}$$

$$s_z = -1.151\sqrt{\frac{k_H}{k_V}}\frac{h}{L_{1/2}}\log\left[\frac{\pi r_w}{h}\left(1+\sqrt{\frac{k_V}{k_H}}\right)\sin\frac{\pi z_w}{h}\right] \quad \text{……..……..…...(2.85)}$$

For late-time radial period that

$$t > \frac{20\phi\bar{\mu}_g c_t L_{1/2}^2}{0.0002637 k_H} \quad \text{……...……...…(2.86)}$$

we have

$$q_g = \frac{p_i^2 - p_{wf}^2}{1424\bar{Z}\bar{\mu}_g T\left[\frac{1.151}{k_H h}\left[\sqrt{\frac{k_H t}{\phi\bar{\mu}_g c_t L_{1/2}^2}} - 2.5267\right] + \frac{s_z}{k_H h} + \frac{s}{2L_{1/2}\sqrt{k_H k_V}}\right]} \quad \text{…..…...(2.87)}$$

$$s_z = -1.151\sqrt{\frac{k_H}{k_V}}\frac{h}{L_{1/2}}\log\left[\frac{\pi r_w}{h}\left(1+\sqrt{\frac{k_V}{k_H}}\right)\sin\frac{\pi z_w}{h}\right] - \frac{k_H}{k_V}\frac{h^2}{2L_{1/2}}\left(\frac{1}{3} - \frac{z_w}{h} + \frac{z_w^2}{h^2}\right) \quad \text{..(2.88)}$$

CHAPTER III

RESULTS AND DISCUSSION

3.1 Introduction

Using the reservoir inflow model, the wellbore pressure drop model, and the solution of the integrated reservoir and wellbore model introduced in Chapter II, we conduct a study on the performance of hydraulic fractured horizontal wells. This study should be designed to follow a rigorous schematic: before a multiple fractures system is developed, we should first study the parameters of a single fracture, and design a single fracture that has the optimum performance. The parameters study should also be conducted in a logical order: before one parameter is examined, all the other parameters must be fixed already; and we find its isolated influence and combined influence with other parameters. Only after the single fracture study is finished, can we perform the multiple fractures study so that each fracture in the system has optimum performance. In the multi-fracture system, each fracture is not independent with each other, the sum of their optimum performance does not necessarily means the performance of the whole system is optimum because the fractures are inter-related in both the reservoir model and the wellbore model. Any fracture as a source influences the reservoir inflow of all others, and the fractures are connected with a wellbore resulting in a relationship of the pressure distribution. Also, fracture distribution influences both the reservoir inflow and the pressure distribution.

A hypothetical reservoir is used as the basic case for this study. The input of the example is shown as Table 3.1 and Fig. 3.1.

Table 3.1 Base data for reservoir, fluid, wellbore, and fracture

Reservoir Data		
Reservoir Length, a	4000	ft
Reservoir Width, b	2000	ft
Reservoir Thickness, h	246	ft
Horizontal Permeability in x-direction, k_x	0.475	md
Horizontal Permeability in y-direction, k_y	0.475	md
Vertical Permeability in z-direction, k_z	0.475	md
Reservoir Pressure, p_i	2335.1	psi
Reservoir Temperature, T	145.8	^oF
Porosity, ϕ	0.09	
Fluid Properties		
Viscosity, μ_g	0.0156	cp
Specific Gravity of Gas, γ_g	0.709	
Total Compressibility, c_t	0.0006	psi^{-1}
Deviation Factor, Z	1	
Roughness, ε	0.0006	
Wellbore Data		
Diameter, D	2.259	inch
Wellbore Flowing Pressure, p_{wf}	1885.5	psi
Well Length	4000	ft
Fracture Data		
Total Volume, V_f	183.708	ft^3
Width, x_f	0.01	ft

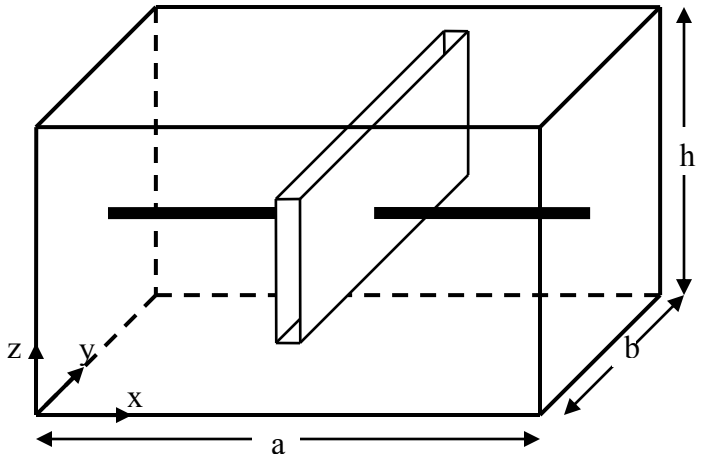

Fig. 3.1 Reservoir, wellbore, and fracture geometry

3.2 Well Placement and Fracture Orientation

Well and fracture orientation can have a great impact on production. A complete study on different patterns of well placement and fracture orientation is necessary before a field is developed. The first problem is to place the fracture. Usually, if fracturing is for vertical communication in case of low vertical permeability, a longitudinal fracture is performed (Fig. 3.2a); if fracturing is for extended reservoir contact, a fracture should be placed perpendicular to the direction that has the greater permeability in a box-shaped reservoir, or perpendicular to the direction that has the greater length if the reservoir is homogenous. The next problem comes how to place the horizontal well when the orientation of the fracture is fixed. The horizontal well can be placed so that the fracture is longitudinal (Fig. 3.2a) or transverse (Fig. 3.2b). Because we want to develop multiple fractures so that production can be enhanced, we need to decide the optimal number of fracture that yields maximum recovery.

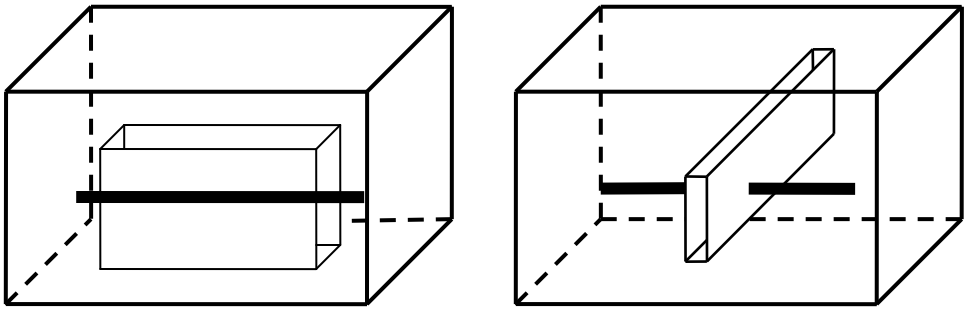

a. Longitudinal b. Transverse

Fig. 3.2 Longitudinal and transverse fracture

3.2.1 The Effect of Reservoir Size on Fracture Orientation

The advantage of fracture orientation in Fig. 3.2b over Fig. 3.2a can also be illustrated by quantitative calculation. The first comparison is performed between the two types of fracture orientation in a 4000 ft by 2000 ft by 246 ft reservoir. Then the ratio of length and width is increased by increasing the length to be 8000 ft. The testing condition is in Table 3.2 and the results are shown in Fig. 3.3. We can see that in the 8000 ft by 2000 ft by 246 ft reservoir, the advantage is amplified. The production from the longitudinal fracture remains almost the same, while production from the transverse fracture increases to some extent. It means that the orientation of fracture is important to well performance, especially for reservoirs with great length-to-width ratio.

Table 3.2 Data for studying the effect of reservoir geometry

	Reservoir Length ,ft	Reservoir Width ,ft	Fracture Geometry
Case 1	4000	2000	longitudinal
Case 2	4000	2000	transverse
Case 3	8000	2000	longitudinal
Case 4	8000	2000	transverse

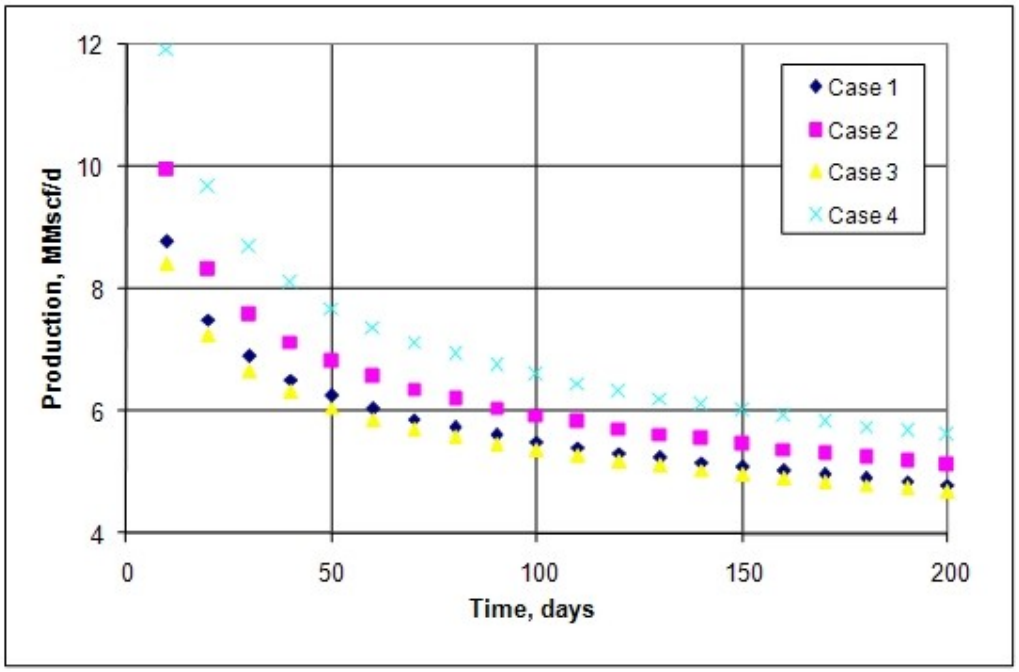

Fig. 3.3 Production history for different fracture orientation

3.2.2 The Effect of Horizontal Permeability on Fracture Orientation

Reservoir geometry is not the only condition we should consider for determining fracture orientation. Reservoir permeability, especially horizontal permeability, is also an important parameter for consideration. We choose the design as in Fig. 3.2b not only because the drainage area is greater in this way, but also based on the fact the reservoir is isotropic in x-y plane. However, if the reservoir is anisotropic, especially when $k_x < k_y$, the advantages of this design would be diminishing. This is because when the fracture is design as in Fig. 3.2b, the main flow will be in x-direction, so if k_x is low, flow in this direction would be restriced. A test shows this by comparing the results of eight cases. The condition of the cases is in Table 3.3, and the results are shown in Fig. 3.4.

Table 3.3 Data for studying the effect of horizontal permeability

	Reservoir Length, ft	Reservoir Width, ft	k_x, md	k_y, md	Fracture Geometry
Case 1	4000	2000	0.475	0.475	longitudinal
Case 2	4000	2000	0.475	0.475	transverse
Case 3	4000	2000	0.35	0.475	longitudinal
Case 4	4000	2000	0.35	0.475	transverse
Case 5	4000	2000	0.25	0.475	longitudinal
Case 6	4000	2000	0.25	0.475	transverse
Case 7	4000	2000	0.15	0.475	longitudinal
Case 8	4000	2000	0.15	0.475	transverse

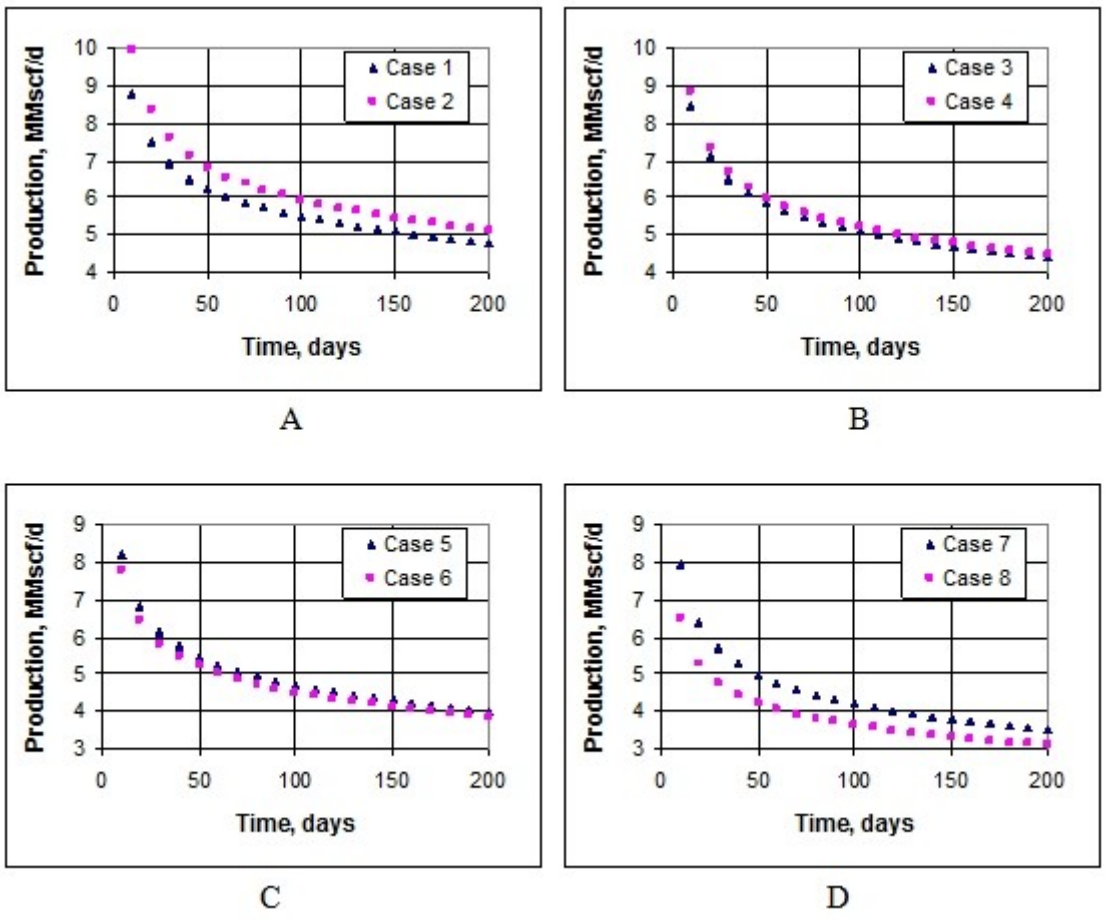

Fig. 3.4 Production history for different horizontal permeability k_x

We can see the flow rate difference between Case 2 over Case 1 (longitudinal fracture vs. transverse fracture) as in Fig. 3.4A becomes smaller in Fig. 3.4B. As k_x decreases further, this advantage is lost completely and the fracture that has smaller drainage area produces more. These facts show that the permeability perpendicular to the fracture plane is also an important parameter to production.

In Fig. 3.4C, the two cases almost have the same production. Notice that in these two cases, k_x is about half of k_y, and reservoir length a doubles width b, so the product of permeability and length in the x and y direction is almost the same. Based on this fact, our first guess is that the production of a fracture is related to the product permeability and length in the direction perpendicular to the fracture plane. The following study is performed to test this guess. In each case, the permeability-to-length product is kept same in two horizontal directions. Input is in Table 3.4, results are shown in Fig. 3.5. Three kinds of results might be lead to: if the two fracture designs result in quite close production, then the permeability-to-length product would be a key factor to determine fracture orientation. If the design in Fig. 3.2a results in much greater production, then permeability would be a parameter of more importance than reservoir geometry. But if the design in Fig. 3.2b results in much greater production, then reservoir geometry would be more important.

Table 3.4 Data for studying the effect of the permeability-to-length product

	a, ft	b, ft	k_x, md	k_y, md	Fracture Geometry
Case 1	6000	2000	0.16	0.48	longitudinal
Case 2	6000	2000	0.16	0.48	transverse
Case 3	8000	2000	0.12	0.48	longitudinal
Case 4	8000	2000	0.112	0.48	transverse
Case 5	7500	1500	0.1	0.48	longitudinal
Case 6	7500	1500	0.1	0.48	transverse

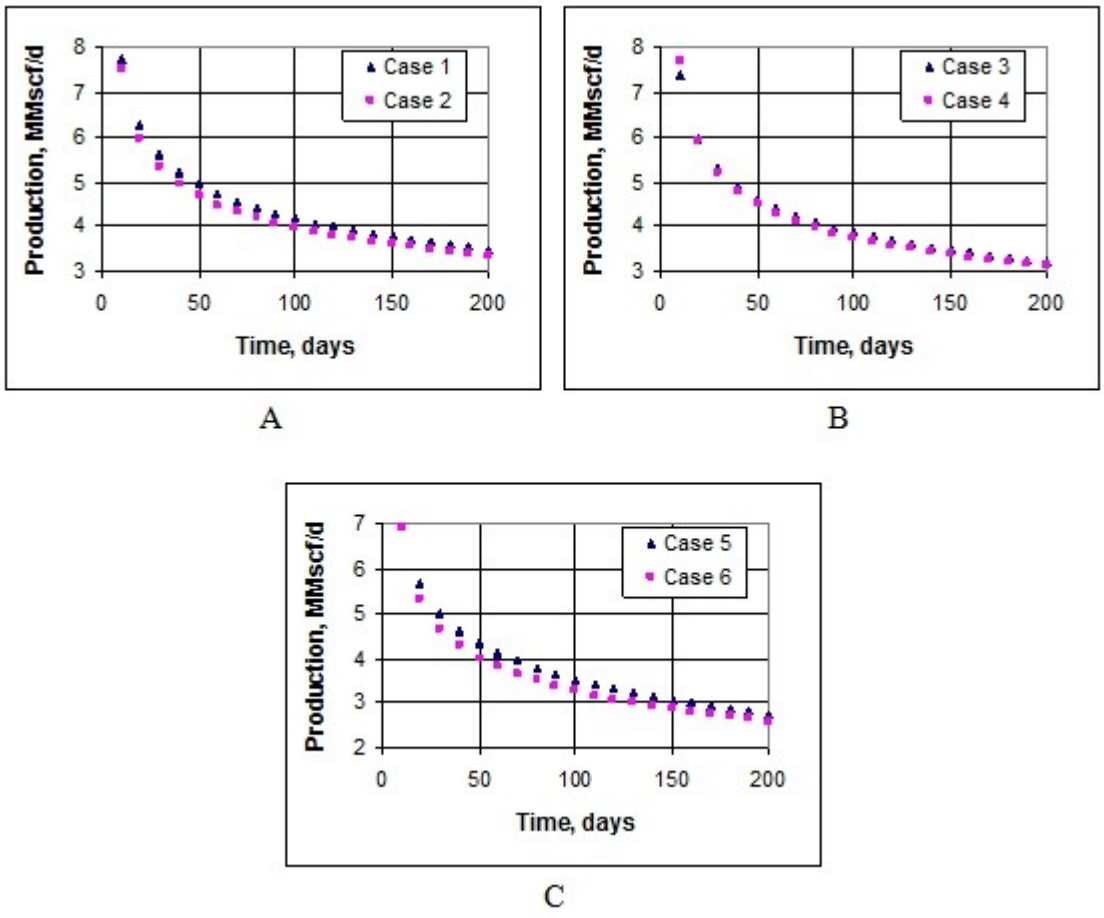

Fig. 3.5 Production history for different permeability-to-length product

Results show that when the product of permeability and reservoir length in the two horizontal directions is the same, the orientation of fracture does not have much influence on production. Further, it is noticed that in all cases the design in Fig. 3.2a leads to a little greater production. This means that horizontal permeability is a little more important parameter than reservoir geometry. Our strategy is that if the permeability-to-length product is much greater in one direction, then we choose this direction to be perpendicular to the fracture plane; if the product is quite close, we choose the direction that has a greater permeability to be perpendicular to the fracture plane.

3.3 The Effect of Fracture Location

Besides fracture orientation, other fracture properties that may have influence on well performance such as fracture location. The following test is conducted based on the basic data for studying the effect of the fracture location. Input is in Table 3.5, results are shown in Figs. 3.6 and 3.7. We can see that at all time, the fracture which is located in the half point of the direction perpendicular to the fracture plane has a greater productivity index. But there appears a “flat region”, especially for early times: productivity remains almost the same for a certain region with the half point at the center, and the region becomes smaller as times goes on. Outside the flat region, productivity is lower as the boundaries are approaching. This is due to the boundary effect, which affects productivity if fluids reach the boundaries. At early times, most of the parts in the reservoir have not reached the boundaries, so the flat region is big. But as time goes on,

more parts reach the boundaries, productivity is decreased as a result, and the flat region becomes smaller.

For our field case, the productivity index is almost kept in the region from 1000 ft to 3000 ft. This fact is important to the design of fracture distribution in the multi-fracture system, because when a fracture is placed further downstream within the flat region, the fracture pressure will decrease due to the pressure drop in the wellbore, and the difference between reservoir pressure and fracture pressure, Δp, will increase. When productivity index is constant, a higher Δp means a higher production.

In the second case, we lower the horizontal permeability and observe a greater flat region (from 500 ft to 3500 ft) as in Fig. 3.6, so we can place the fracture downstream furthermore. However, even if the fracture is placed beyond the flat region, it does not necessarily mean that it is not the optimum design. Although productivity is lower outside the flat region, the location of the fracture is further toward downstream, Δp may be higher as a result. Whether production increases or decreases needs to be further investigated case by case.

Table 3.5 Data for studying the effect of fracture location

	k_x, md	k_y, md	k_z, md
Case 1	0.475	0.475	0.475
Case 2	0.25	0.25	0.475

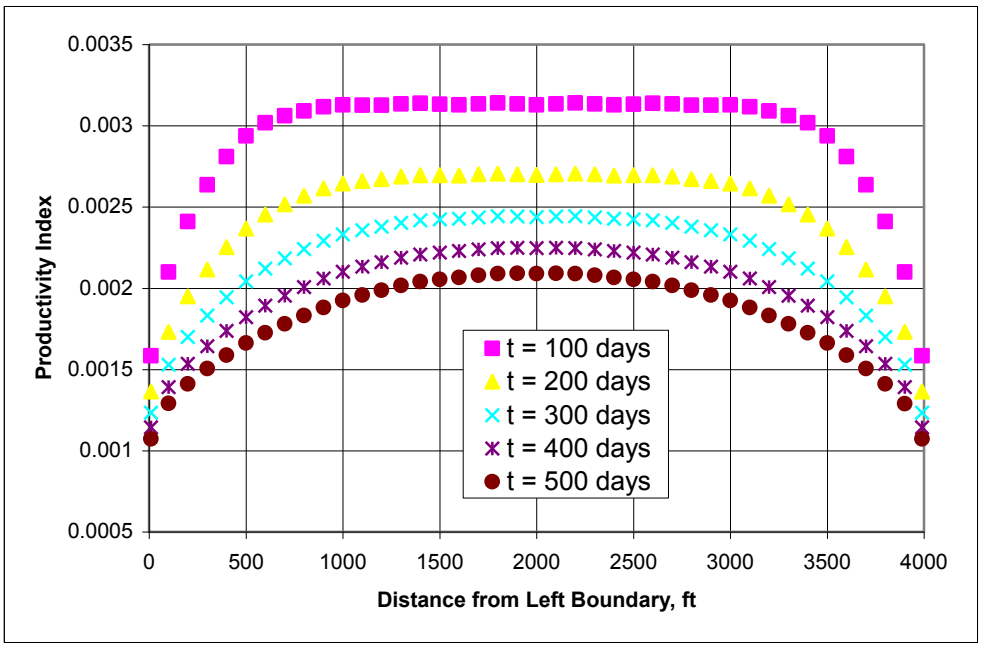

Fig. 3.6 The effect of fracture location, Case 1

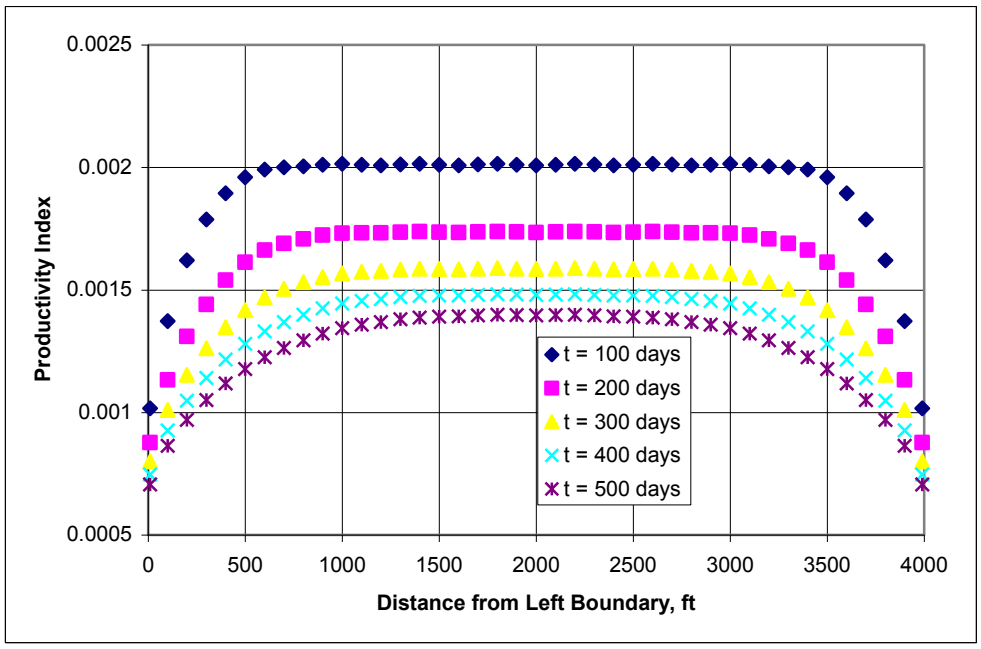

Fig. 3.7 The effect of fracture location, Case 2

3.4 Design of Two-fracture Systems

For a system of multiple fractures, the optimum performance includes two aspects, the optimum design of each single fracture, and the optimum inter-fracture relationships. For the former aspect, we apply the designs concluded in Sections 3.2 and 3.3. Each optimal fracture in the system is a prerequisite for the optimum performance of the whole system, and we can further optimize performance by studying the inter-fracture relationships, which incorporates fracture distribution within the reservoir and the pressure distribution along the wellbore. The inter-fracture relationship study starts from systems of two fractures.

3.4.1 Upstream Performance versus Downstream Performance

Compared to a single fracture, there are more relationships needed for consideration in a system of multiple fractures. First, besides the independent productivity index (PI) for any single fracture, the inter-fracture PI should be calculated to account for the contribution of pressure drop from other fractures. Second, as the fractures are connected by a wellbore, the pressure of different fractures is closely related. Due to the pressure drop along the wellbore, the pressure distribution is never constant. A mathematical expression of the relationship of a two-fracture system is:

$$\begin{bmatrix} A_{11} & A_{12} \\ A_{21} & A_{22} \end{bmatrix} \begin{bmatrix} q_1 \\ q_2 \end{bmatrix} = \begin{bmatrix} p_e^2 - p_1^2 \\ p_e^2 - p_2^2 \end{bmatrix} \quad \text{……(3.1)}$$

$$p_2^2 = p_1^2 - \Delta p^2 \quad \text{……(3.2)}$$

We conduct a study on the comparative performance of the upstream and downstream fracture. Input data is given in Table 3.6, results are shown in Figs. 3.8 and 3.9. In this system, the pressure of the downstream fracture p_2 is lower than upstream one p_1, which is controlled constant, due to the pressure drop along the wellbore segment between the two fractures, Δp. Thus, the difference between the reservoir pressure and the fracture pressure for the downstream fracture, $p_e - p_2$, is higher than $p_e - p_1$. For our case of compressible gas flow, this difference is more significant because the pressure square term, $p_e^2 - p_1^2$ and $p_e^2 - p_2^2$, is used instead. Therefore, production from the downstream fracture q_2 is greater, as shown in Fig. 3.8. However, as the well continues to produce, the advantage of the downstream fracture over the upstream one becomes smaller. This is because all of the coefficients A_{11}, A_{12}, A_{21}, and A_{22} (the inverse of productivity index) will increase as time goes, causing both q_1 and q_2 to decrease. The decrease of q_1 will cause Δp to drop . As p_2 comes close to p_1, q_2 will be quite close to q_1.

Table 3.6 Data for studying upstream and downstream performance

	Fracture Center		
	x_c, ft	y_c, ft	z_c, ft
Fracture 1 (upstream)	3000	1000	123
Fracture 2 (downstream)	1000	1000	123

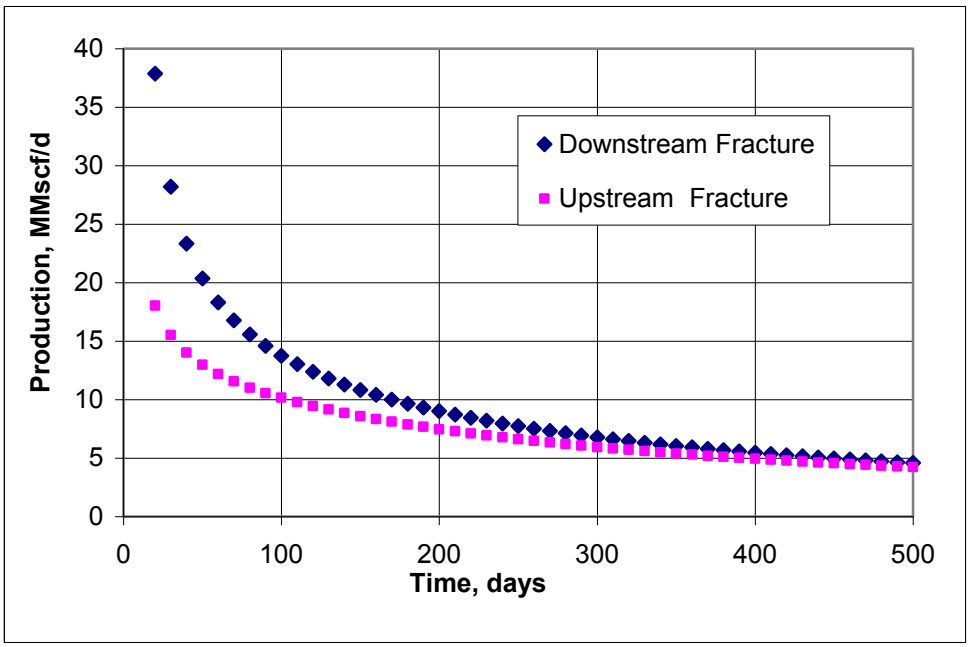

Fig. 3.8 Upstream performance versus downstream performance

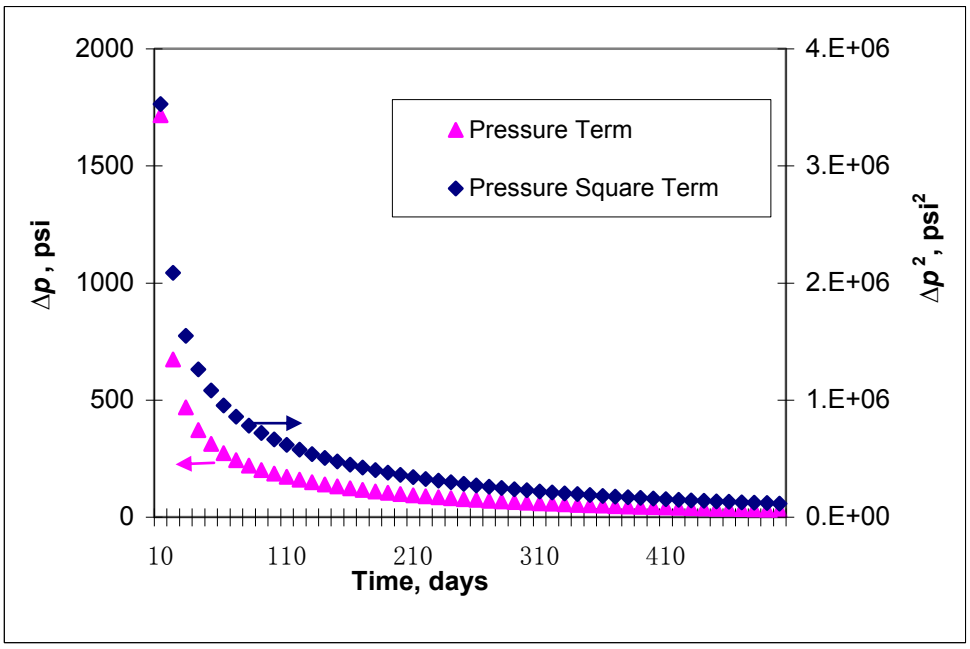

Fig. 3.9 Pressure drop along the wellbore segment between two fractures

3.4.2 Fracture Distribution

Fracture distribution influences the whole system in two aspects: the locations of fractures determine productivity coefficients, and the distance between fractures L influences the pressure drop along the wellbore Δp^2. Since Δp^2 is proportional to L, we hope to enlarge L as much as possible. But if we place the fractures outside the flat region or even at the two ends, the independent productivity coefficients will increase a lot, production will probably also decrease though L is large enough to have a great Δp^2 in this case. The following test studies the influence of L. Input data is given in Table 3.7, results are shown in Figs. 3.10 to 3.12.

Table 3.7 Fixed properties of the upstream fracture

Pressure, psi	Location, ft	Time, days
1885.5	3000	200

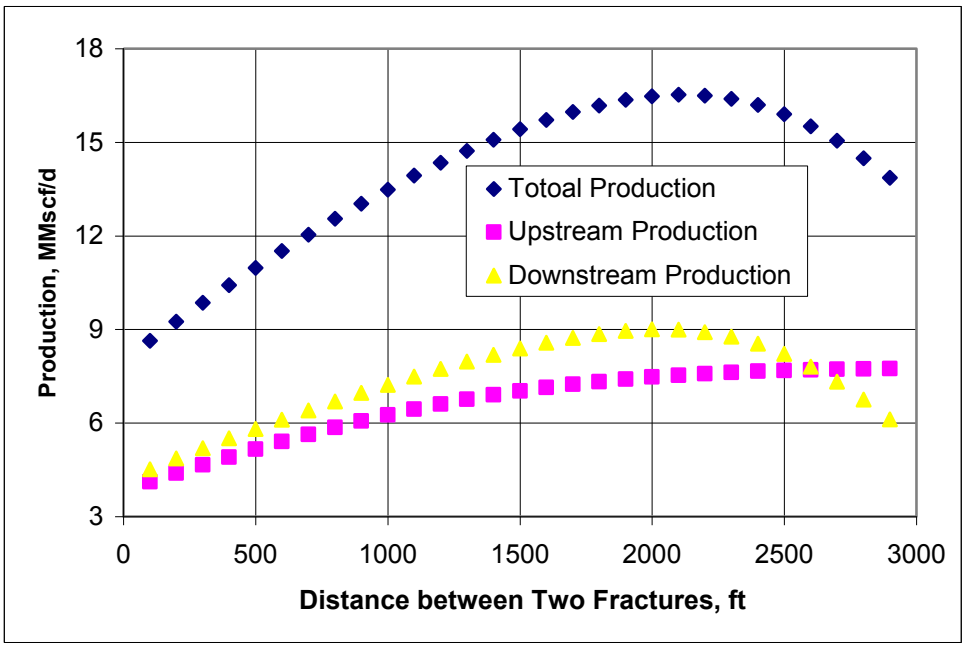

Fig. 3.10 Production history for different distributions

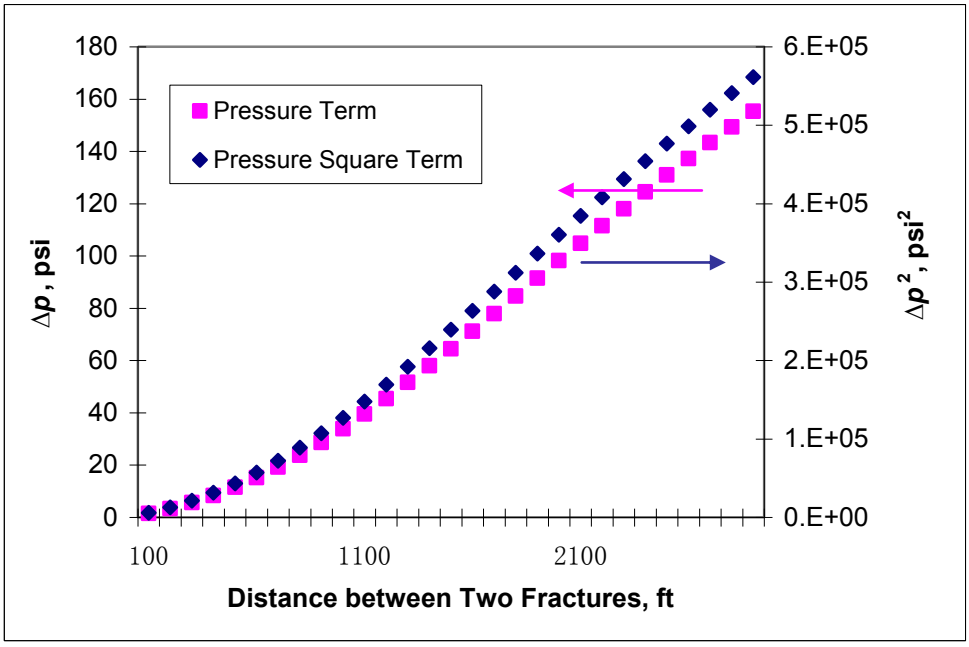

Fig. 3.11 Pressure drop for different distributions

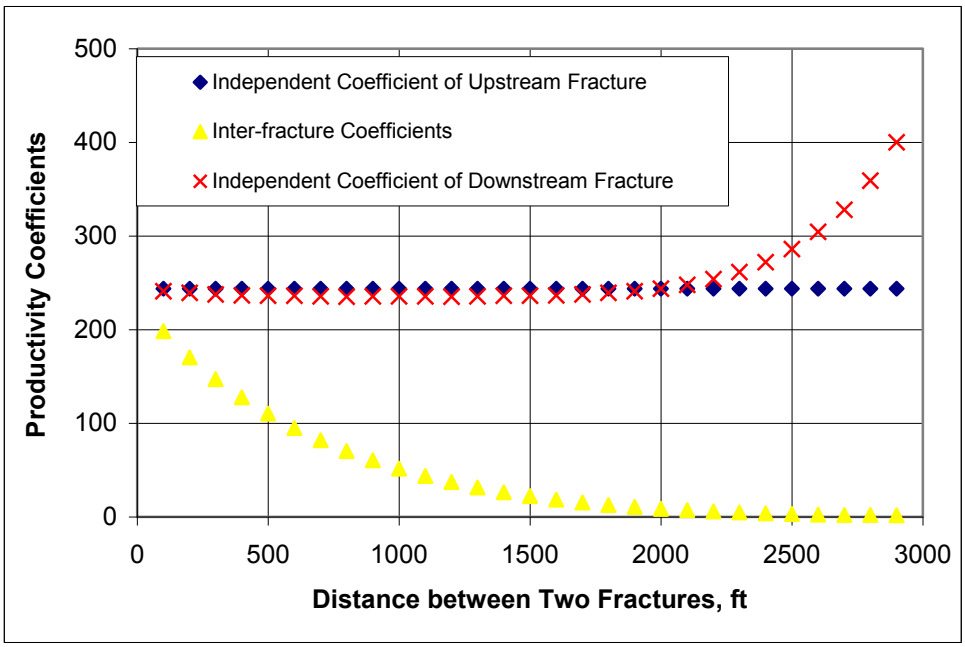

Fig. 3.12 Productivity coefficients for different distributions

When the downstream fracture is located from 1000 to 3000 ft ($0 < L < 2000$ ft) and goes farther from the upstream one, production from both fractures keeps increasing. This is because in this region, the independent coefficients A_{11} and A_{22} remain almost constant and the inter-fracture coefficients A_{12} and A_{21} continue to decrease as shown in Fig. 3.12, and Δp^2 keeps increasing as shown in Fig. 3.11, leading to a greater $p_e^2 - p_2^2$. From Eq. 3.1, it is easy to see that both q_1 and q_2 will increase.

However, when the downstream fracture is located less than 1000 ft ($L > 2000$ ft) and comes closer to the left boundary, total production drops. Actually, the drop is mostly contributed by the decrease of the downstream fracture, while production from the upstream one remains almost unchanged. The reason is that in this region, A_{12} and A_{21} are quite close to zero, meaning that the two fractures have little influence on each

other. For the upstream fracture, its location and pressure is fixed, so A_{11} and $p_e^2 - p_1^2$ is also unchanged. At the same time, A_{22} increases dramatically, at a greater extent than the increase of $p_e^2 - p_2^2$, causing q_2 to decrease. This fact shows that the productivity coefficients, especially the independent ones, are also important to the performance of the whole system. For the upstream fracture fixed at 3000 ft, the best location of the downstream is to place it at about 1000 ft. However, we cannot say that the location of the upstream is optimum. We conduct a test on all possible locations of both fractures, and acquire the following optimum distribution (Table 3.8) from Fig. 3.13.

Table 3.8 Optimum distribution of two-fracture systems

		Location, ft
Upstream	Fracture 1	3000
Downstream	Fracture 2	900

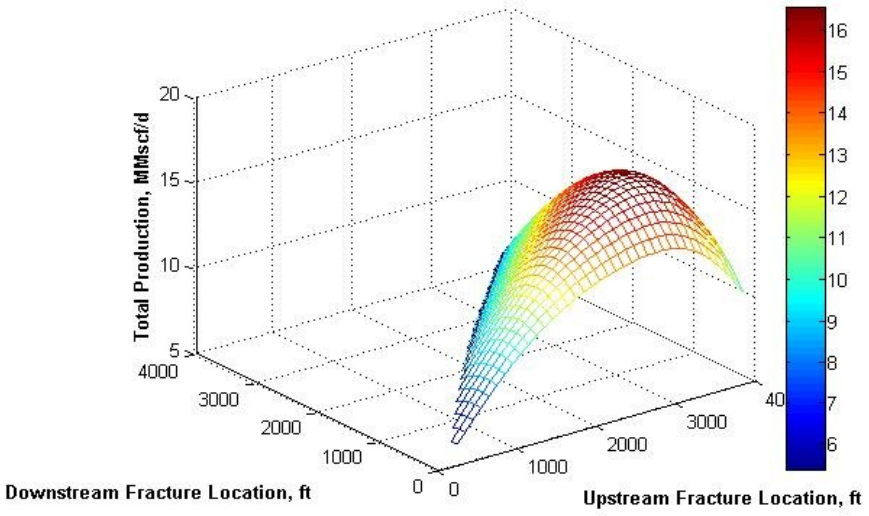

Fig. 3.13 A complete trial on fracture distributions

3.4.3 Wellbore Size

Another parameter that influences the whole performance is wellbore diameter. Actually it does not have any effect on the reservoir model, and only influence the wellbore pressure drop. From Eq. 2.50, Δp^2 is inversely proportional to D^5, meaning that a small change in D can cause a significant change in Δp^2. When Δp^2 is comparable to $p_e^2 - p_1^2$, different values of D will lead to great difference of performance of the whole system. But for our case, $p_e^2 - p_1^2 \sim 10^6$, while $\Delta p^2 \sim 10^5$ or even 10^4. Therefore, even a great change of D does not have significant influence on p_2 (Fig. 3.14). This is also illustrated in the overall performance (Fig. 3.15). Compared with Section 3.4.2, we see that fracture distribution is more sensitive than wellbore pressure drop, or generally, the reservoir model is dominating over the wellbore model in well performance.

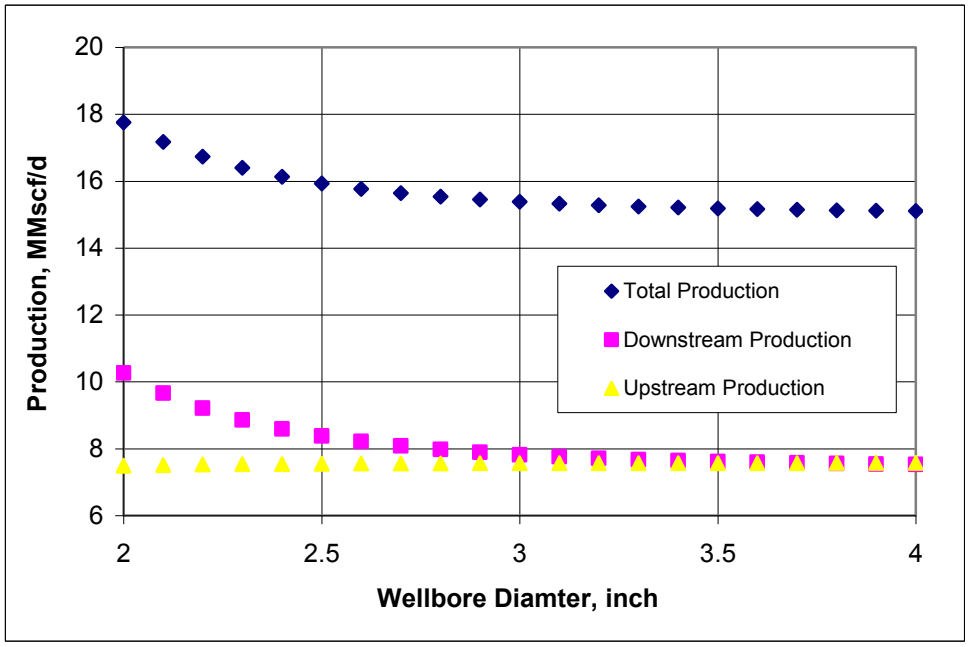

Fig. 3.14 Production history for different wellbore diameters

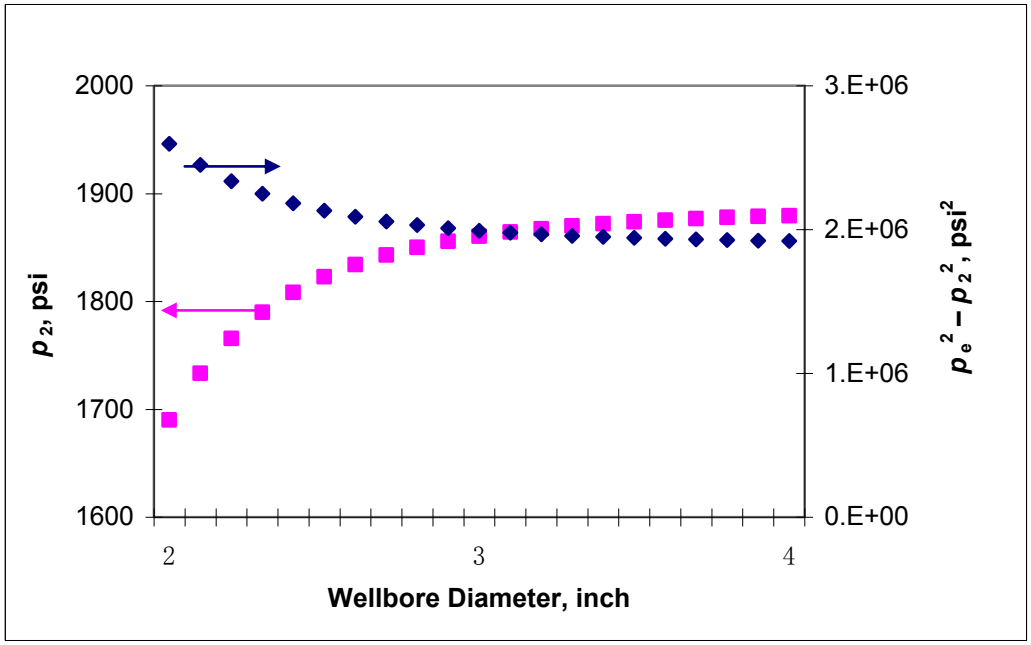

Fig. 3.15 Pressure drop for different wellbore diameters

3.5 Design of Multi-fracture Systems

Since the pressure drop between the wellbore segments of any neighboring fractures is proportional to the square of the total inflow of the upstream fractures, pressure drop in the downstream segment can be much greater than the upstream one. We hope to find the optimum designs of fracture distribution for a fixed number of fractures to maximize the flow rate. However, as the number of fractures increases, total inflow will also increase and wellbore pressure drop will increase too. It is possible that wellbore pressure will drop to be almost zero before flowing to the end of the wellbore. In this case, the fracture towards the heel of the well will contribute to the most of the production, leaving other fractures under-performed. For our basic data that wellbore

diameter is 2.259 inch, this will happen. But we hope to keep the advantage of the optimum distribution, so we place a wellbore with a bigger diameter of 4 inch.

3.5.1 Optimum Distribution for Systems with Fixed Number of Fractures

Similarly to the test on the distribution of two-fracture systems, we have found the optimum distribution for systems with more fractures, shown in Table 3.9. For a homogeneous horizontal permeability, the fractures should be placed evenly. And no matter what the size of each fracture is, the optimum distribution is the same as long as each fracture is of the same size.

Table 3.9 Optimum distributions of multi-fracture systems

Fracture Number	Fracture Location (ft) Downstream ← Upstream									
3	500	2000	3400							
4	400	1500	2600	3500						
6	200	900	1700	2400	3100	3700				
8	200	700	1300	1800	2400	2900	2400	3800		
10	200	600	1000	1400	1800	2200	2600	3000	3400	3800

We see that for multi-fracture system with optimum production, fractures are almost evenly distributed, but not strictly evenly distributed. The distance between neighboring fractures in the upstream part is a litter bigger than the distance in the downstream part. This is due to the wellbore pressure, which causes the pressures at each fracture to be different. But for a system without horizontal well and only fractures, the optimum distribution would be strictly even.

3.5.2 Optimum Number of Fractures

A system with more fractures does not mean a higher total production at all times. At early flowing time, the drainage area of each fracture is small and separated from others, so total drainage area, and furthermore, total production rate, is proportional to the number of fractures. But as time goes on, the drainage area will expand so as to reach the boundaries or overlap with each other. In the end, the total drainage area will almost be the same for systems with different number of fractures since the reservoir is fixed and the drainage area reaches its limit. When adding a new fracture does not lead to a significant increase in flow rate, it should be stopped. For the example in Fig. 3.16, a six-fracture system is very close to 7 or 8 fracture case. If considering the cost, this could be the optimized design. In order to consider the actual number of fracture invested in a more strict way, we need to perform an NPV calculation. We need to know the cost of developing one fracture with certain volume and the current price of gas, and find the number of fracture with the greatest NPV. In this study, we only give a general prediction based on production.

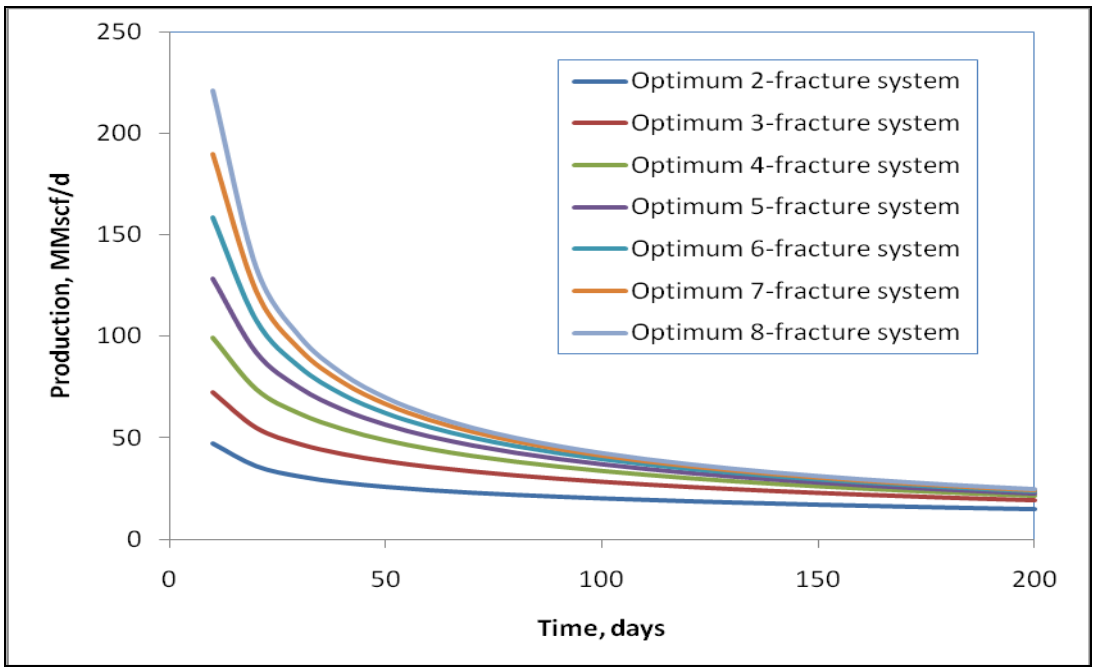

Fig. 3.16 Production history for systems with different number of fractures

3.5.3 Wellbore Pressure Distribution

When we place a fully penetrated horizontal well with a diameter of 4 inch, we have a reasonable pressure drop along the wellbore, and each fracture has almost the same contribution to the total production. Even if we develop a 8-fracture system, the total pressure drop from the upstream end to the downstream end is only about 200 psi at the early flowing time. As time goes, individual production will decrease, and pressure everywhere at the wellbore will increase. The detailed pressure distributions of multi-fracture systems with different number of fractures are illustrated from Figs. 3.17 to 3.23.

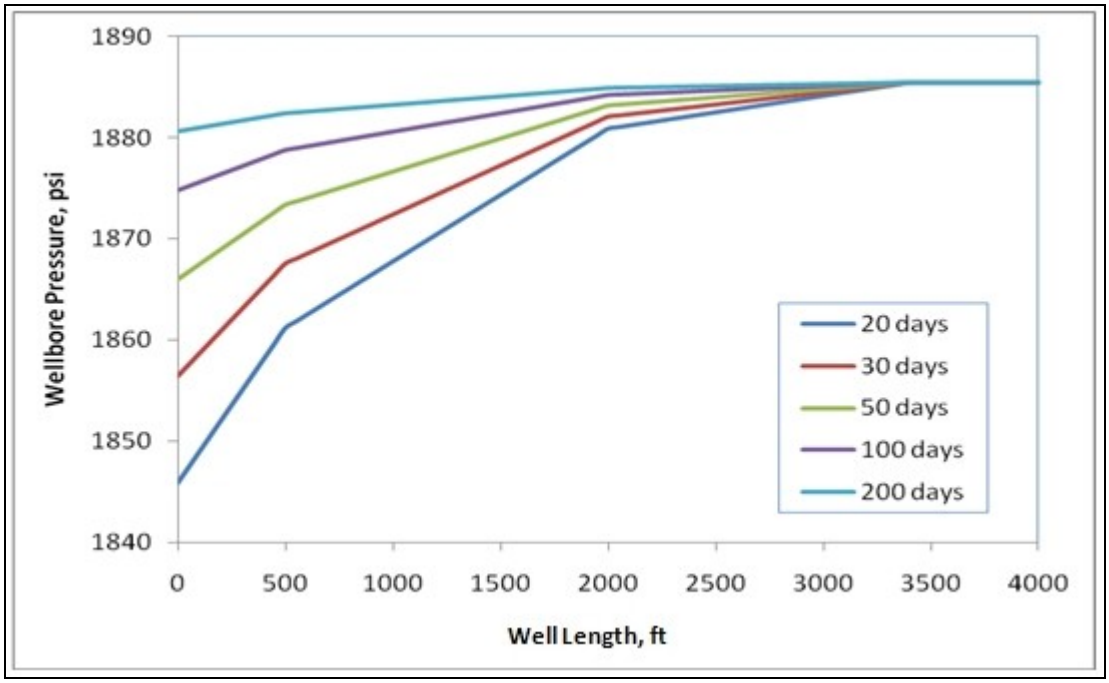

Fig. 3.17 Wellbore pressure distribution for 3-fracture system

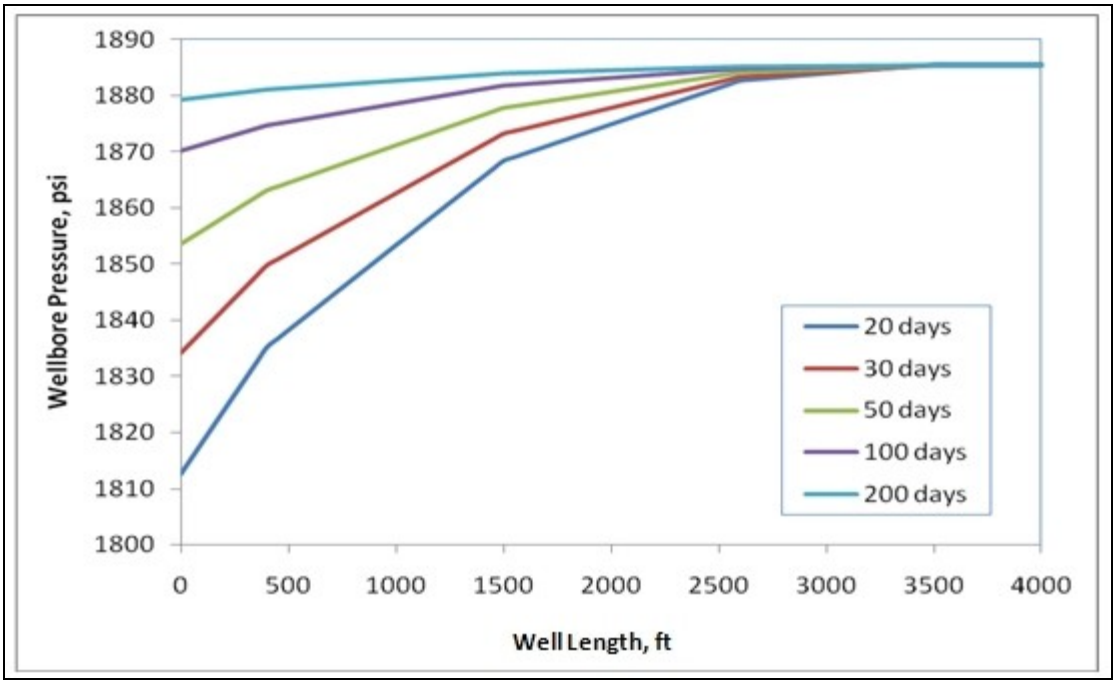

Fig. 3.18 Wellbore pressure distribution for 4-fracture system

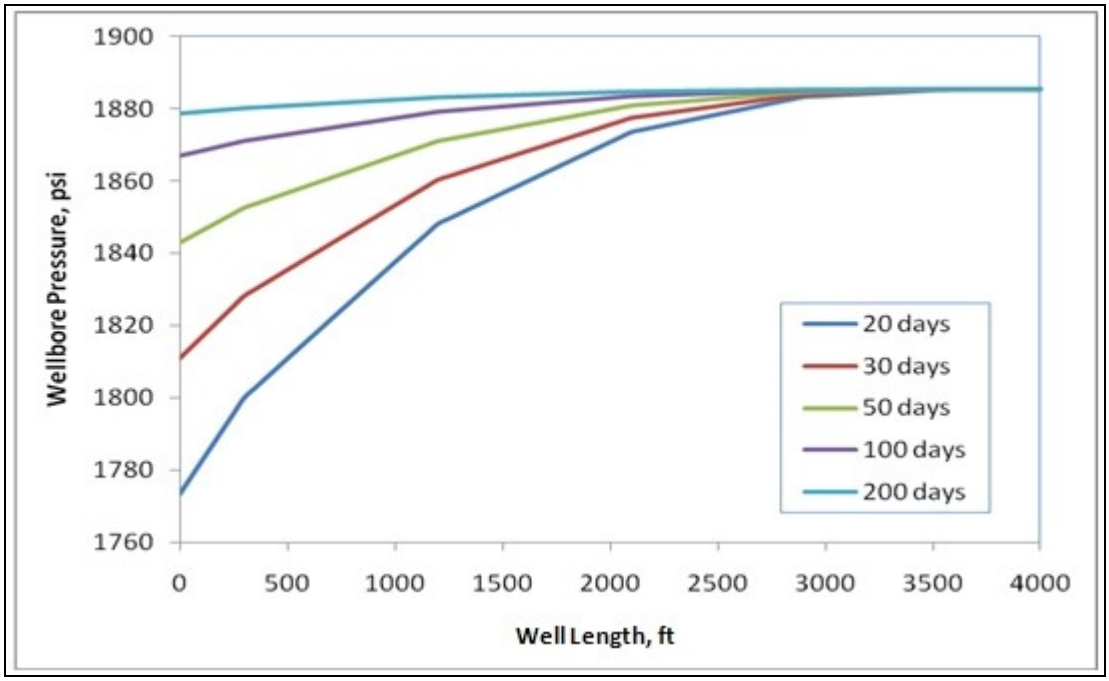

Fig. 3.19 Wellbore pressure distribution for 5-fracture system

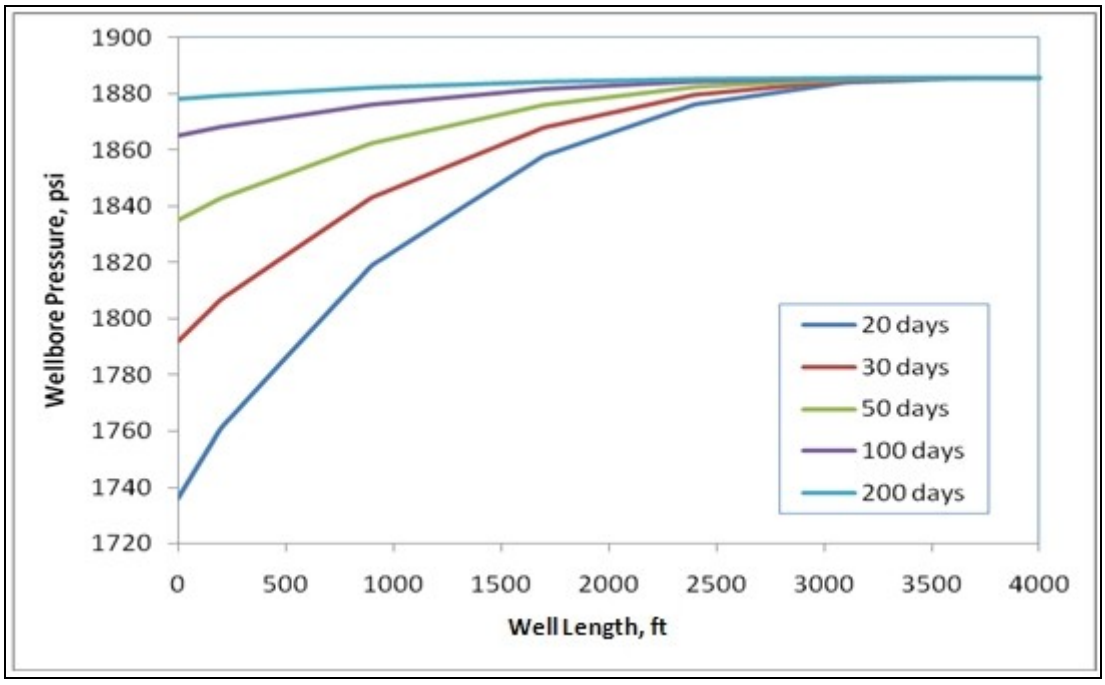

Fig. 3.20 Wellbore pressure distribution for 6-fracture system

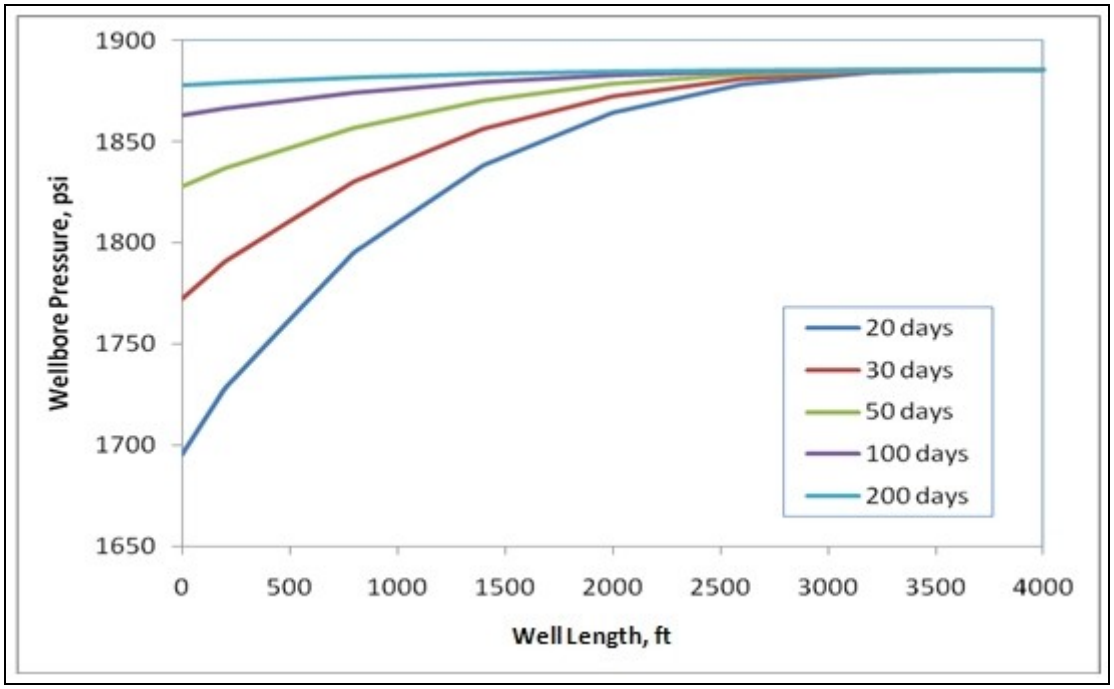

Fig. 3.21 Wellbore pressure distribution for 7-fracture system

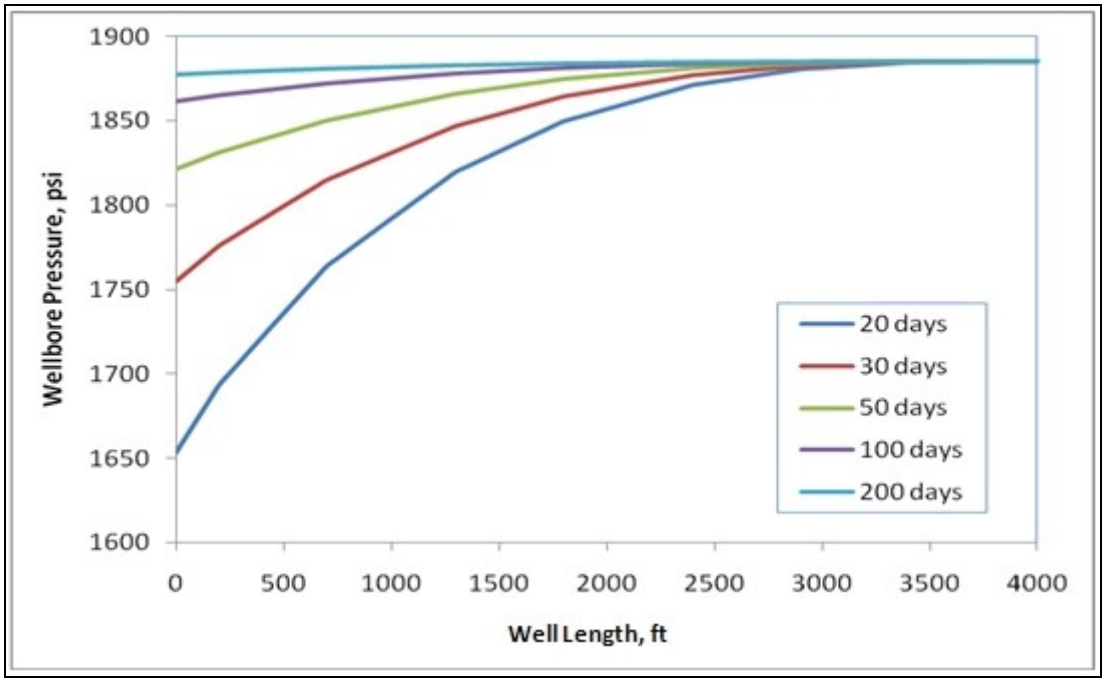

Fig. 3.22 Wellbore pressure distribution for 8-fracture system

3.6 Sum of the Test Procedure

The procedure of fracture design from this study can be summarized in Fig. 3.23.

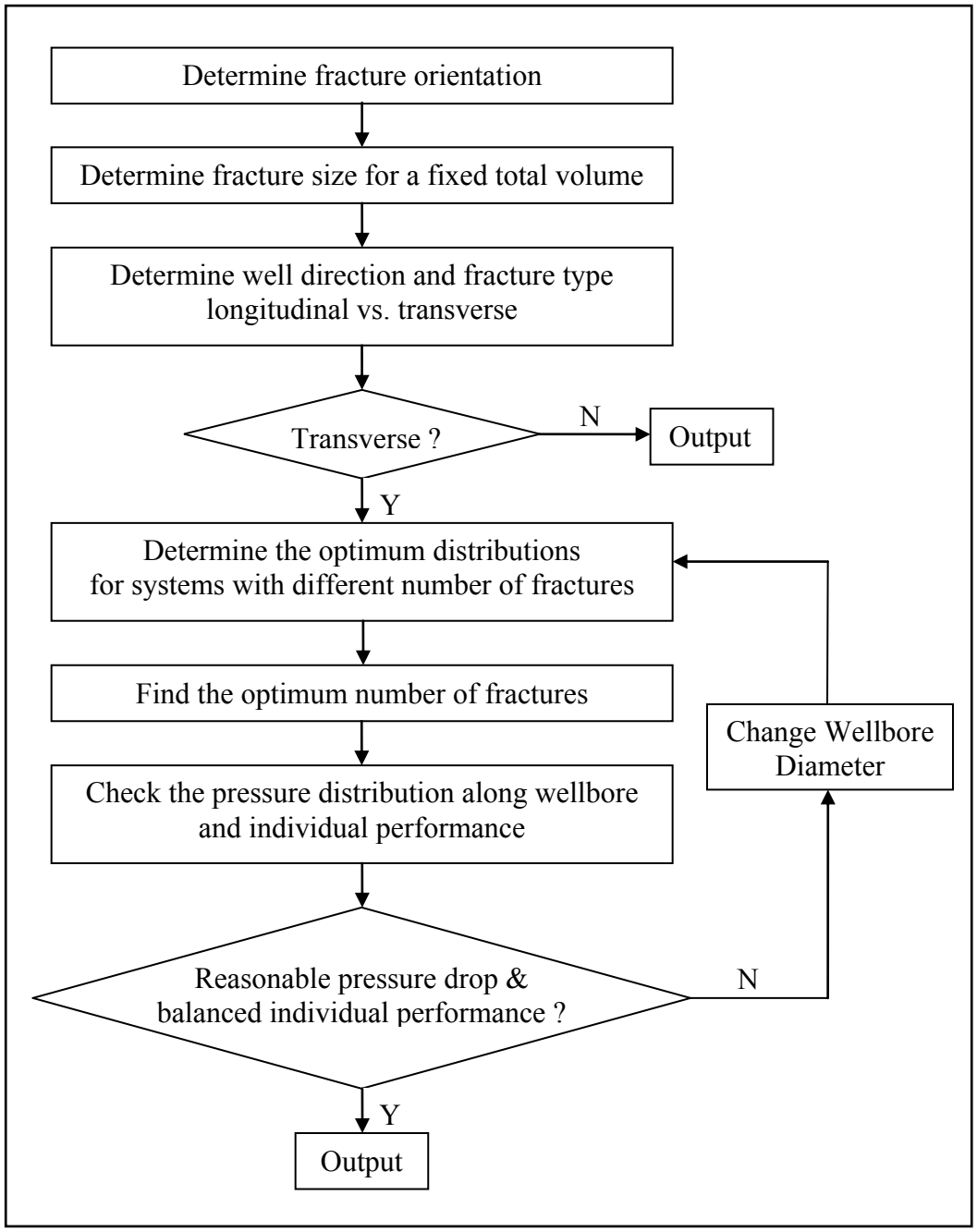

Fig. 3.23 The procedure for field develop with hydraulic fracturing

3.7 Multiple Fractures with Openhole Completion

The discussions in all of the above sections in this chapter are under the case of cased/perforated completion. We performed a thorough study on parameters and gave a complete explanation on production and pressure distribution. In this section, we focus on the case of horizontal well with multiple transverse fractures and openhole completion. Compared to the case of cased/perforated completion, openhole completion brings much more complex relationships: the inter-source productivity index is not only fracture-to-fracture, but also fracture-to-wellbore. As fracture and wellbore are different types of sources (fracture is plane source, wellbore is line source), it becomes difficult to establish this inter-relationship. In order to model the case of openhole completion and get a quick idea whether openhole completion will improve production compared to cased/perforated completion, we need to simply the problem and make certain assumptions as follows.

First, within each wellbore segment, flow from reservoir into wellbore is only through the middle point of the segment. But we treat the whole segment as a line source. Second, there is no reservoir inflow between the center of wellbore segment and the center of fracture (Fig. 3.24). Reservoir inflow has only two paths: through the middle point of segment, and through fracture and its center. Third, for any point along the wellbore, each segment as a line source only influences the pressure at points inside the segment, and has no influence on the points outside it because the line source and the point are on the same line.

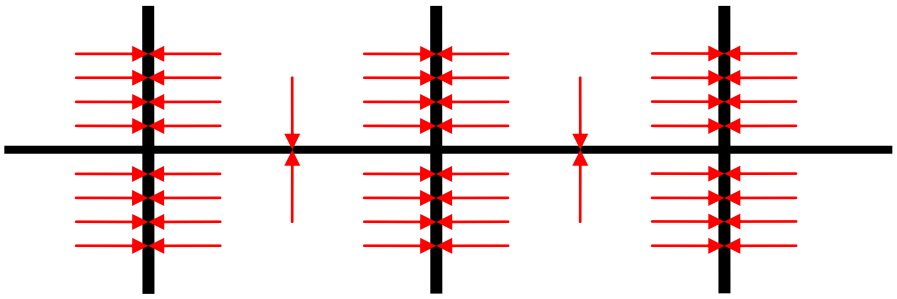

Fig. 3.24 Simplified reservoir inflow

Based on these assumptions, we perform a study on the case of openhole completion hoping to find the comparative production from fractures and wellbore segments, and the comparative performance of different types of completion.

3.7.1 Two-Fracture System Study

Input is given in Table 3.10, results are shown in Figs. 3.25 and 3.26.

Table 3.10 Data for two-fracture system study

Wellbore Data		
Diameter, D	4	inch
Wellbore Flowing Pressure at Toe, p_{wf}	1885.5	psi
Well Length	4000	ft
Fracture Data		
Number of Fractures	2	
Location of Upstream Fracture	3000	ft
Location of Downstream Fracture	1000	ft

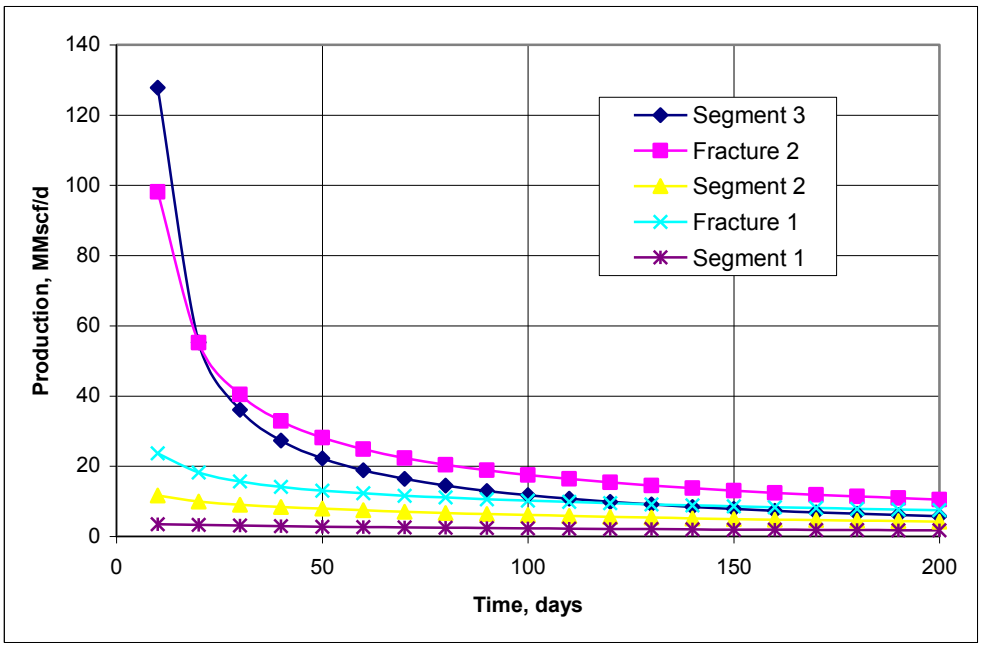

Fig 3.25 Individual performance of a two-fracture system with openhole completion

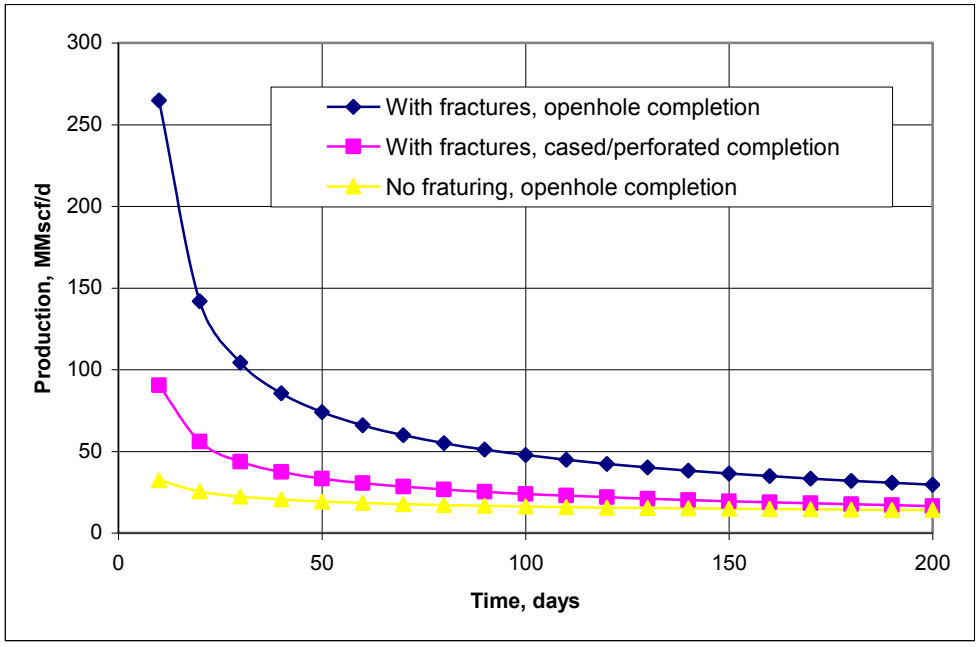

Fig 3.26 Comparative performance for a two-fracture system

3.7.2 Three-Fracture System Study

Input is given in Table 3.11, results are shown in Fig. 3.27.

Table 3.11 Data for three-fracture system study

Fracture Data		
Number of Fractures	3	
Location of Upstream Fracture	3000	ft
Location of Middle Fracture	1500	ft
Location of Downstream Fracture	1000	ft

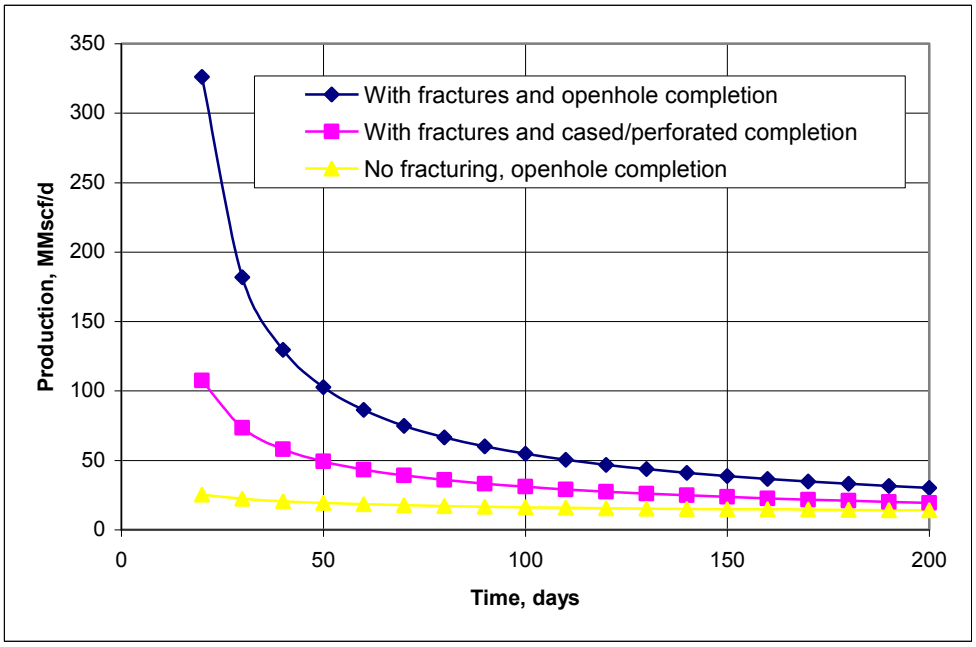

Fig 3.27 Comparative performance for three-fracture system

3.7.3 Four-Fracture System Study

Input is given in Table 3.12, results are shown in Fig. 3.28.

Table 3.12 Data for four-fracture system study

Number of Fractures	4	
Location		
Fracture 1	3200	ft
Fracture 2	2400	ft
Fracture 3	1600	ft
Fracture 4	800	ft

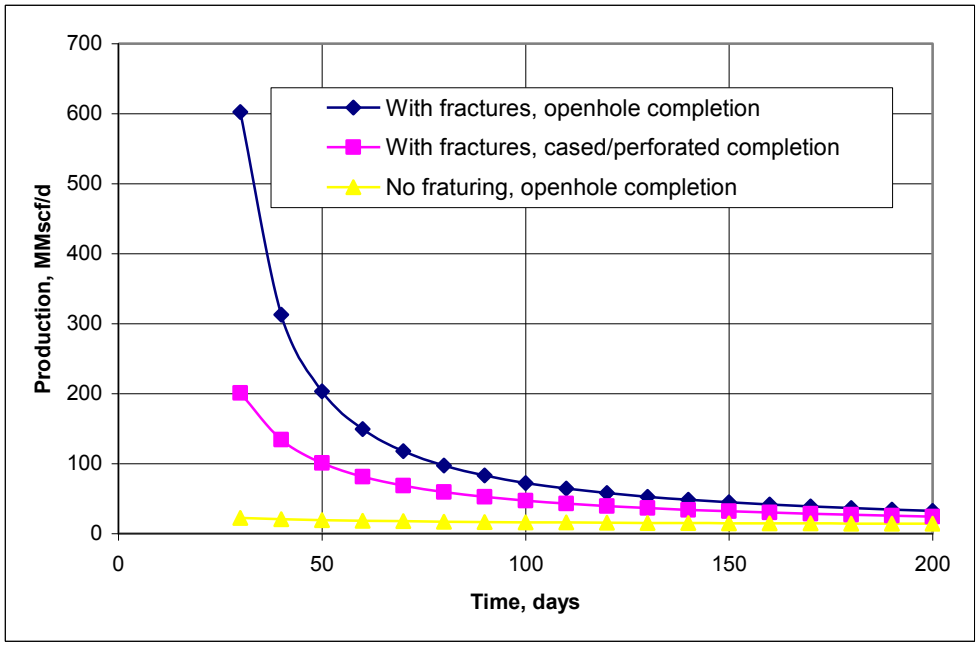

Fig 3.28 Comparative performance for four-fracture system

We can go further by increasing the number of fracture, and the results will be similar: no matter how many fractures we develop, hydraulic fracturing will significantly increase total production compared to openhole/unfractured, and openhole/fractured will lead to even greater production than with cased/perforated/fractured. At the very beginning of the transient flow period, production from openhole/fractured is much

greater than the sum of openhole/unfractured and cased/perforated/fractured. When steady condition is approaching, production from openhole/fractured is almost equal to the sum. By now, we have reached the purpose of studying the performance of openhole/fractured, and do not plan to look into the details, such as pressure distribution along the wellbore and the optimum fracture distribution, due to the simplifications and assumptions mentioned above.

Based on the study in this section, we reach the conclusions that

- Multiple transverse fractures with openhole completion increases reservoir contact and production to the greatest extent, and it is the optimum choice for field development with hydraulic fracturing.
- Production (openhole/fractured) >>

  Production (openhole/unfractured) + Production (cased/perforated/fractured)

  at the beginning of transient flow period.
- Production (openhole/fractured) ≈

  Production (openhole/unfractured) + Production (cased/perforated/fractured)

  when steady condition is approaching.

CHAPTER IV

CONCLUSIONS

4.1 Summary

An integrated reservoir and wellbore model has been established to study the performance of horizontal wells with multiple transverse hydraulic fractures in tight gas reservoirs. The fundamentals of both the reservoir model and the wellbore model have been introduced, the derivation of the final equations that describe the multi-fracture systems has been presented in detail, and a method that rigorously solves the equations has been described.

Compared with previous studies on the performance of fractured horizontal wells, the reservoir model is almost the same: we apply the Green's source functions to calculate reservoir inflow at the presence of fractures as sources in a box-shaped reservoir. However, there's an important improvement that it considers the wellbore pressure drop between the upstream and downstream fractures. Only the pressure of the horizontal well toe is controlled constant, and the pressure distribution along the whole well is calculated by the wellbore pressure drop model.

A rigorously procedure has been proposed for the development of fields with the technology of hydraulic fracturing. First, determine the orientation of fractures. Second, determine the size of fractures if the total volume is fixed. Third, determine the type of fractures (longitudinal or transverse), in other words, determine the direction of horizontal well. Fourth, determine the optimum distributions of systems with different

number of fractures starting from one, if we choose to develop transverse fractures. Fifth, find the optimum number of fractures. Sixth, check the pressure distributions along the wellbore for all of the systems, and change the wellbore diameter if possible to acquire a reasonable pressure distribution and a balanced individual performance. Seventh, repeat the fifth step if a change of wellbore diameter is needed.

Some reservoir, wellbore, and fracture parameters have been studied to discover any underlying principles. We wish to propose some general strategies for developing a field with hydraulic fracturing instead of conducting the procedure for any specific case. The influence of reservoir size and horizontal permeability on fracture orientation and locations, the influence of vertical permeability on fracture size for a fixed total volume, and the influence of wellbore diameter on pressure distribution and individual performance have been explained. Some principles have been presented based on these studies.

It is indicated that fractures should be oriented to have the biggest drainage area, or mathematically, perpendicular to the direction that has the biggest permeability-to-length product. For a homogeneous reservoir or reservoirs with a comparatively large vertical permeability, we should develop longer fractures with a fixed total volume to increase production. Results show that when vertical permeability decreases, the advantage of longer fractures will be weakened or diminish. It is also indicated that a transverse-fracture system is better than a longitudinal fracture because we can have more fractures, so we should place the horizontal well perpendicular to the fracture plane. Also, the optimum location of a single transverse fracture and the optimum distributions

of multiple transverse fractures systems have been found, and results show that the fractures are distributed symmetric and within a region in which the productivity index is high. It is also indicated that total production will not increase when enough fractures are already place, so we should find an optimum number of fractures to avoid further unprofitable investment.

4.2 Recommendations

In this thesis, we studied the performance of three different types of field development, i.e. horizontal well with no hydraulic fracturing and openhole completion, horizontal well with multiple transverse fractures and cased/perforated completion, and horizontal well with multiple transverse fractures and cased/perforated completion. The first two types are completely studied, but the last one is much more complex to completely study so far. The model selected in this thesis for modeling the performance of fractured horizontal well with openhole completion is not the most accurate one: the productivity coefficients caused by wellbore segments as sources are calculated from the expressions for horizontal gas well inflow performance relationship, not from the integration of source functions, because the specific form of source function for a horizontal line source is not available so far; the gas well inflow performance relationship we used is under steady-state condition, while the calculation of productivity coefficients caused by fractures as sources is based on transient condition, so the flow regime is not consistent for fractures and wellbore segments, which is impossible; we also assume that the flow from reservoir into wellbore segment is only through the middle point of the segment

and use the basic pressure drop model, however, the fact is that reservoir inflow is uniform along the segment and Ouyang et al..'s model is more accurate. Therefore, the result is only a approximation. We can only tell whether the production of fractured horizontal well with cased/perforated completion is higher or lower than the production of fractured horizontal well with openhole completion, but cannot tell the accurate production and the pressure distriution along the wellbore in this case.

Due to the above deficiencies, we propose the following tasks for future work:

- Find the specific expression of source function for horizontal line source and incorporate it into the equations for multi-fracture systems.
- Accurately model the fracture-to-wellbore relationship
- Accurately model the reservoir inflow and the pressure distribution within wellbore segments
- Give a more accurate prediction of production.
- Find the optimum distributions of fractures
- Look into details of the inter-source productivity index and pressure distribution, discuss the underlying reasons for different performance.

NOMENCLATURE

A	drainage area
A_{ij}	inter-fracture productivity between the *i*-th and the *j*-th fracture
B_g	gas formation volume factor
c_H	shape factor in Babu and Odeh's horizontal well inflow model
c_t	total compressibility
D	wellbore diameter
$Dp(q)$	pressure drop function
$\vec{F}(\vec{q})$	a set of equations with respect to $\vec{q}$
$\vec{F}'$	Jacobian matrix of $\vec{F}$
$F_{o,w}$	Forchheimer number
f_f	usual friction factor
f_f^*	inflow friction factor
$f_i(\vec{q})$	the *i*-th component of $\vec{F}(\vec{q})$
f_t	turbulence scale factor
f_{tp}	turbulence scale factor for perforated completion
f_{tSL}	turbulence scale factor for slotted liner completion
$f_{tSL,l}$	linear part of turbulence scale factor for slotted liner completion
$f_{tSL,r}$	radial part of turbulence scale factor for slotted liner completion
g	gravity acceleration
g_c	gravitational constant
I_{ani}	anisotropy ratio
k	permeability

k_s	damaged permeability
L	wellbore length
$L_{1/2}$	wellbore half length
L_p	perforation length
L_{pD}	dimensionless perforation length
$L_{pD,eff}$	effective dimensionless perforation length
L_s	wellbore segment length
MW	molecular weight
m_s	number of slot units around a circumference of a liner
N_{Re}	usual reynolds number
$N_{\mathrm{Re},w}$	inflow reynolds number
n_s	number of slots in a slot unit
p	pressure
$\bar{p}$	average pressure
p_{sc}	pressure at standard condition
p_{wf}	bottom-hole flowing pressure
q	flow from reservoir into fracture
$\vec{q}$	flow vector
q_I	flow from reservoir into wellbore
R	universal gas constant
r_{pD}	dimensionless perforation radius
r_w	wellbore radius
s	skin factor
s^0	rate-independent skin factor
s_{2D}	2D perforation skin factor

s_{3D}	3D perforation skin factor
s_{3D}	3D perforation skin factor
s_d^o	openhole damaged skin factor
s_p	perforation skin factor
s_p^0	rate-independent perforation skin factor
s_{SL}	slotted liner skin factor
s_{SL}^0	rate-independent slotted liner skin factor
$s_{SL,l}^0$	linear part of rate-independent slotted liner skin factor
$s_{SL,r}^0$	radial part of rate-independent slotted liner skin factor
s_{wb}	wellbore blockage perforation skin component
s_R	partial penetration skin
s_z	vertical-direction skin factor
T	temperature
$\overline{T}$	average temperature
T_{sc}	temperature at standard condition
u	velocity in the pipeline
W_s	shaft work
w_s	slot width
w_{sD}	dimensionless slot width
x_p	perforation spacing
x_{pD}	dimensionless perforation spacing
Z	deviation factor
$\overline{Z}$	average deviation factor
z_w	height from bottom to horizontal wellbore

Greek

$\alpha^{'}$, $\alpha^{"}$	perforation angle parameter
β	non-darcy coefficient
β_d	non-darcy coefficient for damaged zone
γ_g	specific gravity of gas
$\delta\vec{q}^{(k)}$	upgrading step at the *k*th step
ε	roughness
θ	angle between pipeline and horizon
μ	viscosity
$\bar{\mu}$	average viscosity
ρ	density
ϕ	porosity

Superscript

k	the *k*th Step in Newton-Raphson iteration
o	openhole
0	rate-independent

Subscript

D	dimensionless
g	gas
H	horizontal
l	linear
o	oil
N	number of fractures
p	perforation
r	radial
SL	slotted liner

sc	standard conditions
t	total
V	vertical
w	wellbore
x	x-direction
y	y-direction
z	vertical direction

REFERENCES

Babu, D.K. and Odeh, A.S. 1989. Productivity of a Horizontal Well. *SPERE* **5** (2), 254-255. SPE-20394-PA.

Butler, R.M. 1994. *Horizontal Wells for the Recovery of Oil, Gas, and Bitumen*, Monograph No. 2, Petroleum Soc. Of Canadian Institute of Mining, Metallurgy, and Petroleum.

Chen, N.H. 1979. An Explicit Equation for Friction Factor in Pipe. *Ind. Eng. Chem. Fund*. **18** (3):296-297

Economides, M.J., Deimbachor, F.X., Brand, C.W., and Heinemann, Z.E. 1991. Comprehensive Simulation of Horizontal-Well Performance. *SPEFE* **6** (4): 418-426. SPE-20717-PA.

Economides, M.J., Hill, A.D., and Ehlig-Economides, C. 1993. *Petroleum Production Systems.* Eaglewood Cliffs, New Jersey: Practice-Hall Inc.

Furui, K. 2004. A Comprehensive Skin Factor Model for Well Completions Based on Finite Element Simulations. PhD dissertation, University of Texas, Austin.

Furui, K., Zhu, D., and Hill, A.D. 2003. A Rigorous Formation damage Skin Factor and Reservoir Inflow Model for A Horizontal Well. *SPEPF* **18** (3): 151-157. SPE-84964-PA.

Gringarten, A.C. and Ramey, H.J. 1973. The Use of Source and Green's Functions in Solving Unsteady-Flow Problems in Reservoirs. *SPEJ* (October) **285**: 285-295.

Hill A.D., Zhu, D., and Economides, M.J. 2008. *Multilateral Wells*. Richardson, Texas: SPE.

Joshi, S.D. 1988. Augmentation of Well Productivity with Slant and Horizontal Wells. *JPT* **40** (6): 729-739; *Trans.*, AIME, **285**. SPE-15375-PA.

Kamkom, R. 2007. Modeling Performance of Horizontal, Undulating, and Multilateral Wells. PhD dissertation, Texas A&M University, College Station.

Kincaid, D. and Cheney W. 1991. *Numerical Analysis: Mathematics of Scientific Computing*. Pacific Grove, California: Brooks/Cole Pub.

Kuchuk, F.J., Goode, P.A., Wilkinson, D.J., and Thambynayagam, R.K.M. 1991. Pressure-Transient Behavior of Horizontal Wells with and without Gas Cap or Aquifer. *SPEFE* **6** (1): 86-94. SPE-17413-PA.

Lin, J. and Zhu, D. 2010. Modeling Well Performance for Fractured Horizontal Gas Wells. Paper SPE 130794 presented at the International Oil and Gas Conference and Exhibition, Beijing, China, 8-10 June.

Magalhaes, F., Zhu, D., Amini, S., and Valko, P.P. 2007. Optimization of Fractured Well Performance of Horizontal Gas Wells. Paper SPE 108779 presented at the International Oil Conference and Exhibition, Veracruz, Mexico, 27-30 June.

Muskat, M. 1937. *The Flow of Homogeneous Fluids through Porous Media*, 55. New York City: McGraw-Hill Book Co.

Ouyang, L.B., Arbabi, S., and Aziz, K. 1998. General Wellbore Flow Model for Horizontal, Vertical, and Slanted Well Completions. *SPEJ* **3** (2): 124-133. SPE-36608-PA.

Ozkan, E., Raghvan, R., and Joshi, S.D. 1989. Horizontal Well Pressure Analysis. *SPEFE* **4** (4): 567-575. SPE-16378-PA.

Valko, P.P. and Amini, S. 2007. The Method of Distributed Volumetric Sources for Calculating the Transient and Pseudosteady-State Productivity of Complex Well-Fracture Configurations. Paper SPE 106279 presented at the SPE Hydraulic Fracturing Technology Conference, 29-31 January.

.

APPENDIX A

SOURCE FUNCTIONS

The reservoir model is briefly introduced in this appendix. Reservoir gas flow under transient condition in a homogeneous and anisotropic porous media can be formulated as (Gringarten and Ramey, 1973)

$$\frac{k_x}{\phi\mu c_t}\frac{\partial^2 p^2}{\partial x^2}+\frac{k_y}{\phi\mu c_t}\frac{\partial^2 p^2}{\partial y^2}+\frac{k_z}{\phi\mu c_t}\frac{\partial^2 p^2}{\partial z^2}=\frac{\partial^2 p^2}{\partial t} \quad \text{.....(A.1)}$$

For a rectangular reservoir with a slab source, Eq. A.1 is solved by the use of Green's source functions

$$p_e^2-p^2(x,y,z,t)=\frac{8875.9\overline{ZT}\mu_g q_g}{\alpha x_f y_f z_f}\int_0^t\left(\int_{x_{s1}}^{x_{s2}} S_x(x,\tau;x_s)\,dx_s\right)\left(\int_{y_{s1}}^{y_{s2}} S_y(y,\tau;y_s)\,dy_s\right)\left(\int_{z_{s1}}^{z_{s2}} S_z(z,\tau;z_s)\,dz_s\right)d\tau \quad \text{.....(A.2)}$$

Here, x_f , y_f , and z_f is the width, length, and height of fracture respectively, $(x_{s1},x_{s2})\times(y_{s1},y_{s2})\times(z_{s1},z_{s2})$ is the boundary coordinates of fracture, (x_s,y_s,z_s) is any point within fracture, and $\alpha=\phi\mu c_t$. The choice of source functions is based on reservoir geometry, boundary conditions, and source geometry. For a rectangular reservoir with no flux boundary and a slab source, we select

$$S_x=\frac{x_f}{x_e}\left[1+\frac{4x_e}{\pi x_f}\sum_{n=1}^{\infty}\frac{1}{n}\exp\left(-\frac{n^2\pi^2\eta_x t}{x_e^2}\right)\sin\frac{n\pi x_f}{2x_e}\cos\frac{n\pi x_s}{x_e}\cos\frac{n\pi x}{x_e}\right] \quad \text{.....(A.3)}$$

$$S_y=\frac{y_f}{y_e}\left[1+\frac{4y_e}{\pi y_f}\sum_{k=1}^{\infty}\frac{1}{k}\exp\left(-\frac{k^2\pi^2\eta_y t}{x_y^2}\right)\sin\frac{k\pi y_f}{2y_e}\cos\frac{k\pi y_s}{y_e}\cos\frac{k\pi y}{y_e}\right] \quad \text{.....(A.4)}$$

$$S_z = \frac{z_f}{z_e}\left[1+\frac{4z_e}{\pi z_f}\sum_{n=1}^{\infty}\frac{1}{l}\exp\left(-\frac{l^2\pi^2\eta_z t}{z_e^2}\right)\sin\frac{l\pi z_f}{2z_e}\cos\frac{l\pi z_s}{z_e}\cos\frac{l\pi z}{z_e}\right] \text{…...……..…(A.5)}$$

VITA

Name: Guangwei Dong

Address: Department of Petroleum Engineering
c/o Dr. Ding Zhu
Texas A&M University
College Station, TX 77843-3116

Email Address: Guangwei.dong@pe.tamu.edu

Education: B.S., Information and Computing Science, Tsinghua University, 2008
M.S., Petroleum Engineering, Texas A&M University, 2010